

Finite-size effects on the behavior of the susceptibility in van der Waals films under $(+;+)$ boundary conditions

Daniel Dantchev^{1,2}, Joseph Rudnick², and M. Barmatz³

¹ Institute of Mechanics – BAS, Academic Georgy Bonchev St. building 4, 1113 Sofia, Bulgaria,

² Department of Physics and Astronomy, UCLA, Los Angeles, California 90095-1547, USA,

³ Jet Propulsion Laboratory, California Institute of Technology, Pasadena, California 91109-8099, USA
(Dated: March 23, 2022)

We study critical point finite-size effects in the case of the susceptibility of a film in which interactions are characterized by a van der Waals-type power law tail. The geometry is appropriate to a slab-like system with two bounding surfaces. Boundary conditions are consistent with surfaces that both prefer the same phase in the low temperature, or broken symmetry, state. We take into account both interactions within the system and interactions between the constituents of the system and the material surrounding it. Specific predictions are made with respect to the behavior of a ^3He and ^4He films in the vicinity of their respective liquid-vapor critical points.

PACS numbers: 64.60.-i, 64.60.Fr, 75.40.-s

I. INTRODUCTION

Confinement to a finite volume introduces a variety of modifications to the behavior of a system in the vicinity of a phase transition. The existence of a single bounding surface leads to surface phase transitions [1, 2, 3], critical adsorption [1, 2], wetting [4] and interface phenomena [5]. The requirement that the system is of finite extent in one or more directions generates effects associated with finite-size scaling theory [6, 7, 8, 9], including shifts in critical points, dimensional crossover, rounding of phase transitions and also to such phenomena as capillary condensation [10] and the interface delocalization phase transition [11, 12].

In addition, the nature of the interaction within the system and between the system and the surrounding world influences leading and sub-leading thermodynamic behavior at and near a critical point [13, 14, 15, 16, 17, 18].

In this article we will discuss finite-size effects as they apply to the susceptibility of a film of a non-polar fluid having a thickness L in which the intrinsic interaction J^1 is of the van der Waals type, decaying with distance r between the molecules of the fluid as $J^1 \sim r^{-(d+1)}$. Here d is the dimensionality of the system while $\gamma > 2$ is a parameter characterizing the decay of the interaction. The film is bounded by a substrate that interacts with the fluid with a similar van der Waals type forces, i.e. of the type $J^{ls} \sim z^{-\gamma}$, where z is the distance from the boundary of the system while $\gamma_s > 2$ characterizes the decay of the fluid-substrate potential. For realistic fluids $d = \gamma = \gamma_s = 3$. The discussion in this paper will be quite general, but we will be principally interested in an Ising type model, which is commonly utilized to represent a non-polar fluid.

As a specific application, we will estimate the parameters required for the prediction of the behavior of the finite-size susceptibility in the case of ^3He and ^4He films near their respective liquid-vapor critical points. In line with an experimental investigation of the phenomena

that we discuss here, we assume that the film is surrounded by gold surfaces. We will take into account both the van der Waals type interaction between the atoms of the ^3He (or ^4He) and the corresponding interaction between the Au atoms and ^3He (or ^4He) atoms.

According to general scaling arguments [2], [19], the finite-size behavior of the susceptibility in a film of a fluid subject to $(+;+)$ boundary conditions is

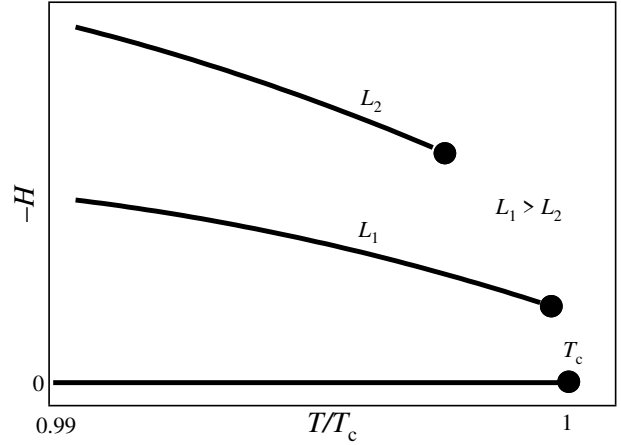


FIG. 1: A schematic (H, T) phase diagram near the critical point of a d -dimensional system with $(+;+)$ boundary conditions [12, 20]. The line $H = 0, T < T_c$ represents the bulk phase coexistence line. (In the case of a fluid system the vertical $-H$ axis then corresponds to the vapor side of the fluid-vapor coexistence curve.) The upper phase coexistence line is for a system with thickness L_2 , while the lower one is for a system with thickness L_1 , where $L_1 > L_2$. Away from the critical region the shift in the phase boundary is proportional to L^{-1} , while within it is proportional to $L^{-\gamma}$. As is shown, the lines of a first-order phase transition (with respect to the external bulk magnetic field) end at critical points of the $(d-1)$ -dimensional system, the positions of which depend on L , on the amplitude of the (long-range) surface field and on the presence or absence of long-range interactions between the spins of the system.

$$\chi(t;h;L) = \chi_{\text{bulk}}(t;h) + L^{-1} [\chi_{\text{surface}1}(t;h) + \chi_{\text{surface}2}(t;h)] = \quad (1.1)$$

$$L^{-1} = X(L = t; a_h h L^{-1} = ; b L^{2-\frac{d+2}{s}}; h_s L^{(d+2-\frac{2}{s})=2-\frac{2}{s}}; a_1 L^{-1});$$

where $\chi_{\text{bulk}}(t;h)$ is the bulk susceptibility, $\chi_{\text{surface}1}(t;h)$ and $\chi_{\text{surface}2}(t;h)$ are the surface susceptibilities, $t(T) = t_1(T - T_c^+; h=0)$, t_0 is the bulk correlation length, $t = (T - T_c)/T_c$ is the reduced temperature, T_c is the bulk critical temperature, t_0^+ , a_h , b , h_w , s and a_1 are nonuniversal metric constants, while ν , ν_1 and

ν_1 are the universal critical exponents for the corresponding short-range system. For a schematic phase diagram in the (H, T) plane of the system see Fig. 1. Assuming $\nu > 2$ and $s > (d+2-\frac{2}{s})=2$, one can expand (1.1), which leads to

$$\chi(t;h;L) = \chi_{\text{bulk}}(t;h) + L^{-1} [\chi_{\text{surface}1}(t;h) + \chi_{\text{surface}2}(t;h)] \quad (1.2)$$

$$+ L^{-1} X^{\text{sr}}(a_t t L^{-1} = ; a_h h L^{-1} = ; a_1 L^{-1}) + h_s L^{(d+2-\frac{2}{s})=2} X_{s;1}^{\text{lr}}(a_t t L^{-1} = ; a_h h L^{-1} =)$$

$$+ L^{-(2+\frac{2}{s})} h_s^2 L^{-(d)} X_{s;2}^{\text{lr}}(a_t t L^{-1} = ; a_h h L^{-1} =) + b X_b^{\text{lr}}(a_t t L^{-1} = ; a_h h L^{-1} =)$$

where X^{sr} is the (universal) scaling function characterizing the truly short-range system, while the remaining part in (1.2) describes the contributions due to the (subleading) long-range part of the interaction. While it is well established that X^{sr} tends to zero as $\exp[-aL^{-1}]$ with a a constant when $L \rightarrow \infty$, the functions $X_{s;1}^{\text{lr}}$, $X_{s;2}^{\text{lr}}$ and X_b^{lr} are expected to decay only in a power-law-in- L way.

Because of that, whenever $L \rightarrow \infty$ the functions $X_{s;1}^{\text{lr}}$, $X_{s;2}^{\text{lr}}$ and X_b^{lr} will determine the leading-in- L finite-size contributions to the susceptibility of the system, and, therefore, the leading finite-size behavior of the susceptibility. Note that due to the lack of χ , χ symmetry in the surface field given $(+, +)$ boundary conditions, one finds in the susceptibility a term linearly proportional to h_w (in addition to the term proportional to h_w^2).

In the case of the "genuine" van der Waals interaction $d = s = 3$. For the three-dimensional Ising model [21] $\nu = 0.034$, $\nu_1 = 1.2385$, $\nu_2 = 0.631$, $\nu_3 = 0.103$, $\nu_4 = 0.329$, $\nu_5 = 0.53$.

In the remainder of this article we will consider only the case of identical substrates bounding the system. That is, we assume $\chi_{\text{surface}1}(t;h) = \chi_{\text{surface}2}(t;h) = \chi_{\text{surface}}(t;h)$. Furthermore, for the bulk susceptibility one has [22]

$$\chi_{\text{bulk}}(t;h) = \chi_{\text{bulk};\text{sr}}(t;h) + \chi_{\text{bulk};\text{lr}}(t;h); \quad (1.3)$$

where [22, 23, 24]

$$\chi_{\text{bulk};\text{sr}}(t;h) = t_0^+ [1 + \nu_1 t + \nu_2 t^2 + \nu_3 t^3 + \nu_4 t^4 + \nu_5 t^5 + \nu_6 t^6 + \nu_7 t^7 + \nu_8 t^8 + \nu_9 t^9 + \nu_{10} t^{10} + \nu_{11} t^{11} + \nu_{12} t^{12} + \nu_{13} t^{13} + \nu_{14} t^{14} + \nu_{15} t^{15} + \nu_{16} t^{16} + \nu_{17} t^{17} + \nu_{18} t^{18} + \nu_{19} t^{19} + \nu_{20} t^{20} + \nu_{21} t^{21} + \nu_{22} t^{22} + \nu_{23} t^{23} + \nu_{24} t^{24} + \nu_{25} t^{25} + \nu_{26} t^{26} + \nu_{27} t^{27} + \nu_{28} t^{28} + \nu_{29} t^{29} + \nu_{30} t^{30} + \nu_{31} t^{31} + \nu_{32} t^{32} + \nu_{33} t^{33} + \nu_{34} t^{34} + \nu_{35} t^{35} + \nu_{36} t^{36} + \nu_{37} t^{37} + \nu_{38} t^{38} + \nu_{39} t^{39} + \nu_{40} t^{40} + \nu_{41} t^{41} + \nu_{42} t^{42} + \nu_{43} t^{43} + \nu_{44} t^{44} + \nu_{45} t^{45} + \nu_{46} t^{46} + \nu_{47} t^{47} + \nu_{48} t^{48} + \nu_{49} t^{49} + \nu_{50} t^{50} + \nu_{51} t^{51} + \nu_{52} t^{52} + \nu_{53} t^{53} + \nu_{54} t^{54} + \nu_{55} t^{55} + \nu_{56} t^{56} + \nu_{57} t^{57} + \nu_{58} t^{58} + \nu_{59} t^{59} + \nu_{60} t^{60} + \nu_{61} t^{61} + \nu_{62} t^{62} + \nu_{63} t^{63} + \nu_{64} t^{64} + \nu_{65} t^{65} + \nu_{66} t^{66} + \nu_{67} t^{67} + \nu_{68} t^{68} + \nu_{69} t^{69} + \nu_{70} t^{70} + \nu_{71} t^{71} + \nu_{72} t^{72} + \nu_{73} t^{73} + \nu_{74} t^{74} + \nu_{75} t^{75} + \nu_{76} t^{76} + \nu_{77} t^{77} + \nu_{78} t^{78} + \nu_{79} t^{79} + \nu_{80} t^{80} + \nu_{81} t^{81} + \nu_{82} t^{82} + \nu_{83} t^{83} + \nu_{84} t^{84} + \nu_{85} t^{85} + \nu_{86} t^{86} + \nu_{87} t^{87} + \nu_{88} t^{88} + \nu_{89} t^{89} + \nu_{90} t^{90} + \nu_{91} t^{91} + \nu_{92} t^{92} + \nu_{93} t^{93} + \nu_{94} t^{94} + \nu_{95} t^{95} + \nu_{96} t^{96} + \nu_{97} t^{97} + \nu_{98} t^{98} + \nu_{99} t^{99} + \nu_{100} t^{100} + \nu_{101} t^{101} + \nu_{102} t^{102} + \nu_{103} t^{103} + \nu_{104} t^{104} + \nu_{105} t^{105} + \nu_{106} t^{106} + \nu_{107} t^{107} + \nu_{108} t^{108} + \nu_{109} t^{109} + \nu_{110} t^{110} + \nu_{111} t^{111} + \nu_{112} t^{112} + \nu_{113} t^{113} + \nu_{114} t^{114} + \nu_{115} t^{115} + \nu_{116} t^{116} + \nu_{117} t^{117} + \nu_{118} t^{118} + \nu_{119} t^{119} + \nu_{120} t^{120} + \nu_{121} t^{121} + \nu_{122} t^{122} + \nu_{123} t^{123} + \nu_{124} t^{124} + \nu_{125} t^{125} + \nu_{126} t^{126} + \nu_{127} t^{127} + \nu_{128} t^{128} + \nu_{129} t^{129} + \nu_{130} t^{130} + \nu_{131} t^{131} + \nu_{132} t^{132} + \nu_{133} t^{133} + \nu_{134} t^{134} + \nu_{135} t^{135} + \nu_{136} t^{136} + \nu_{137} t^{137} + \nu_{138} t^{138} + \nu_{139} t^{139} + \nu_{140} t^{140} + \nu_{141} t^{141} + \nu_{142} t^{142} + \nu_{143} t^{143} + \nu_{144} t^{144} + \nu_{145} t^{145} + \nu_{146} t^{146} + \nu_{147} t^{147} + \nu_{148} t^{148} + \nu_{149} t^{149} + \nu_{150} t^{150} + \nu_{151} t^{151} + \nu_{152} t^{152} + \nu_{153} t^{153} + \nu_{154} t^{154} + \nu_{155} t^{155} + \nu_{156} t^{156} + \nu_{157} t^{157} + \nu_{158} t^{158} + \nu_{159} t^{159} + \nu_{160} t^{160} + \nu_{161} t^{161} + \nu_{162} t^{162} + \nu_{163} t^{163} + \nu_{164} t^{164} + \nu_{165} t^{165} + \nu_{166} t^{166} + \nu_{167} t^{167} + \nu_{168} t^{168} + \nu_{169} t^{169} + \nu_{170} t^{170} + \nu_{171} t^{171} + \nu_{172} t^{172} + \nu_{173} t^{173} + \nu_{174} t^{174} + \nu_{175} t^{175} + \nu_{176} t^{176} + \nu_{177} t^{177} + \nu_{178} t^{178} + \nu_{179} t^{179} + \nu_{180} t^{180} + \nu_{181} t^{181} + \nu_{182} t^{182} + \nu_{183} t^{183} + \nu_{184} t^{184} + \nu_{185} t^{185} + \nu_{186} t^{186} + \nu_{187} t^{187} + \nu_{188} t^{188} + \nu_{189} t^{189} + \nu_{190} t^{190} + \nu_{191} t^{191} + \nu_{192} t^{192} + \nu_{193} t^{193} + \nu_{194} t^{194} + \nu_{195} t^{195} + \nu_{196} t^{196} + \nu_{197} t^{197} + \nu_{198} t^{198} + \nu_{199} t^{199} + \nu_{200} t^{200} + \nu_{201} t^{201} + \nu_{202} t^{202} + \nu_{203} t^{203} + \nu_{204} t^{204} + \nu_{205} t^{205} + \nu_{206} t^{206} + \nu_{207} t^{207} + \nu_{208} t^{208} + \nu_{209} t^{209} + \nu_{210} t^{210} + \nu_{211} t^{211} + \nu_{212} t^{212} + \nu_{213} t^{213} + \nu_{214} t^{214} + \nu_{215} t^{215} + \nu_{216} t^{216} + \nu_{217} t^{217} + \nu_{218} t^{218} + \nu_{219} t^{219} + \nu_{220} t^{220} + \nu_{221} t^{221} + \nu_{222} t^{222} + \nu_{223} t^{223} + \nu_{224} t^{224} + \nu_{225} t^{225} + \nu_{226} t^{226} + \nu_{227} t^{227} + \nu_{228} t^{228} + \nu_{229} t^{229} + \nu_{230} t^{230} + \nu_{231} t^{231} + \nu_{232} t^{232} + \nu_{233} t^{233} + \nu_{234} t^{234} + \nu_{235} t^{235} + \nu_{236} t^{236} + \nu_{237} t^{237} + \nu_{238} t^{238} + \nu_{239} t^{239} + \nu_{240} t^{240} + \nu_{241} t^{241} + \nu_{242} t^{242} + \nu_{243} t^{243} + \nu_{244} t^{244} + \nu_{245} t^{245} + \nu_{246} t^{246} + \nu_{247} t^{247} + \nu_{248} t^{248} + \nu_{249} t^{249} + \nu_{250} t^{250} + \nu_{251} t^{251} + \nu_{252} t^{252} + \nu_{253} t^{253} + \nu_{254} t^{254} + \nu_{255} t^{255} + \nu_{256} t^{256} + \nu_{257} t^{257} + \nu_{258} t^{258} + \nu_{259} t^{259} + \nu_{260} t^{260} + \nu_{261} t^{261} + \nu_{262} t^{262} + \nu_{263} t^{263} + \nu_{264} t^{264} + \nu_{265} t^{265} + \nu_{266} t^{266} + \nu_{267} t^{267} + \nu_{268} t^{268} + \nu_{269} t^{269} + \nu_{270} t^{270} + \nu_{271} t^{271} + \nu_{272} t^{272} + \nu_{273} t^{273} + \nu_{274} t^{274} + \nu_{275} t^{275} + \nu_{276} t^{276} + \nu_{277} t^{277} + \nu_{278} t^{278} + \nu_{279} t^{279} + \nu_{280} t^{280} + \nu_{281} t^{281} + \nu_{282} t^{282} + \nu_{283} t^{283} + \nu_{284} t^{284} + \nu_{285} t^{285} + \nu_{286} t^{286} + \nu_{287} t^{287} + \nu_{288} t^{288} + \nu_{289} t^{289} + \nu_{290} t^{290} + \nu_{291} t^{291} + \nu_{292} t^{292} + \nu_{293} t^{293} + \nu_{294} t^{294} + \nu_{295} t^{295} + \nu_{296} t^{296} + \nu_{297} t^{297} + \nu_{298} t^{298} + \nu_{299} t^{299} + \nu_{300} t^{300} + \nu_{301} t^{301} + \nu_{302} t^{302} + \nu_{303} t^{303} + \nu_{304} t^{304} + \nu_{305} t^{305} + \nu_{306} t^{306} + \nu_{307} t^{307} + \nu_{308} t^{308} + \nu_{309} t^{309} + \nu_{310} t^{310} + \nu_{311} t^{311} + \nu_{312} t^{312} + \nu_{313} t^{313} + \nu_{314} t^{314} + \nu_{315} t^{315} + \nu_{316} t^{316} + \nu_{317} t^{317} + \nu_{318} t^{318} + \nu_{319} t^{319} + \nu_{320} t^{320} + \nu_{321} t^{321} + \nu_{322} t^{322} + \nu_{323} t^{323} + \nu_{324} t^{324} + \nu_{325} t^{325} + \nu_{326} t^{326} + \nu_{327} t^{327} + \nu_{328} t^{328} + \nu_{329} t^{329} + \nu_{330} t^{330} + \nu_{331} t^{331} + \nu_{332} t^{332} + \nu_{333} t^{333} + \nu_{334} t^{334} + \nu_{335} t^{335} + \nu_{336} t^{336} + \nu_{337} t^{337} + \nu_{338} t^{338} + \nu_{339} t^{339} + \nu_{340} t^{340} + \nu_{341} t^{341} + \nu_{342} t^{342} + \nu_{343} t^{343} + \nu_{344} t^{344} + \nu_{345} t^{345} + \nu_{346} t^{346} + \nu_{347} t^{347} + \nu_{348} t^{348} + \nu_{349} t^{349} + \nu_{350} t^{350} + \nu_{351} t^{351} + \nu_{352} t^{352} + \nu_{353} t^{353} + \nu_{354} t^{354} + \nu_{355} t^{355} + \nu_{356} t^{356} + \nu_{357} t^{357} + \nu_{358} t^{358} + \nu_{359} t^{359} + \nu_{360} t^{360} + \nu_{361} t^{361} + \nu_{362} t^{362} + \nu_{363} t^{363} + \nu_{364} t^{364} + \nu_{365} t^{365} + \nu_{366} t^{366} + \nu_{367} t^{367} + \nu_{368} t^{368} + \nu_{369} t^{369} + \nu_{370} t^{370} + \nu_{371} t^{371} + \nu_{372} t^{372} + \nu_{373} t^{373} + \nu_{374} t^{374} + \nu_{375} t^{375} + \nu_{376} t^{376} + \nu_{377} t^{377} + \nu_{378} t^{378} + \nu_{379} t^{379} + \nu_{380} t^{380} + \nu_{381} t^{381} + \nu_{382} t^{382} + \nu_{383} t^{383} + \nu_{384} t^{384} + \nu_{385} t^{385} + \nu_{386} t^{386} + \nu_{387} t^{387} + \nu_{388} t^{388} + \nu_{389} t^{389} + \nu_{390} t^{390} + \nu_{391} t^{391} + \nu_{392} t^{392} + \nu_{393} t^{393} + \nu_{394} t^{394} + \nu_{395} t^{395} + \nu_{396} t^{396} + \nu_{397} t^{397} + \nu_{398} t^{398} + \nu_{399} t^{399} + \nu_{400} t^{400} + \nu_{401} t^{401} + \nu_{402} t^{402} + \nu_{403} t^{403} + \nu_{404} t^{404} + \nu_{405} t^{405} + \nu_{406} t^{406} + \nu_{407} t^{407} + \nu_{408} t^{408} + \nu_{409} t^{409} + \nu_{410} t^{410} + \nu_{411} t^{411} + \nu_{412} t^{412} + \nu_{413} t^{413} + \nu_{414} t^{414} + \nu_{415} t^{415} + \nu_{416} t^{416} + \nu_{417} t^{417} + \nu_{418} t^{418} + \nu_{419} t^{419} + \nu_{420} t^{420} + \nu_{421} t^{421} + \nu_{422} t^{422} + \nu_{423} t^{423} + \nu_{424} t^{424} + \nu_{425} t^{425} + \nu_{426} t^{426} + \nu_{427} t^{427} + \nu_{428} t^{428} + \nu_{429} t^{429} + \nu_{430} t^{430} + \nu_{431} t^{431} + \nu_{432} t^{432} + \nu_{433} t^{433} + \nu_{434} t^{434} + \nu_{435} t^{435} + \nu_{436} t^{436} + \nu_{437} t^{437} + \nu_{438} t^{438} + \nu_{439} t^{439} + \nu_{440} t^{440} + \nu_{441} t^{441} + \nu_{442} t^{442} + \nu_{443} t^{443} + \nu_{444} t^{444} + \nu_{445} t^{445} + \nu_{446} t^{446} + \nu_{447} t^{447} + \nu_{448} t^{448} + \nu_{449} t^{449} + \nu_{450} t^{450} + \nu_{451} t^{451} + \nu_{452} t^{452} + \nu_{453} t^{453} + \nu_{454} t^{454} + \nu_{455} t^{455} + \nu_{456} t^{456} + \nu_{457} t^{457} + \nu_{458} t^{458} + \nu_{459} t^{459} + \nu_{460} t^{460} + \nu_{461} t^{461} + \nu_{462} t^{462} + \nu_{463} t^{463} + \nu_{464} t^{464} + \nu_{465} t^{465} + \nu_{466} t^{466} + \nu_{467} t^{467} + \nu_{468} t^{468} + \nu_{469} t^{469} + \nu_{470} t^{470} + \nu_{471} t^{471} + \nu_{472} t^{472} + \nu_{473} t^{473} + \nu_{474} t^{474} + \nu_{475} t^{475} + \nu_{476} t^{476} + \nu_{477} t^{477} + \nu_{478} t^{478} + \nu_{479} t^{479} + \nu_{480} t^{480} + \nu_{481} t^{481} + \nu_{482} t^{482} + \nu_{483} t^{483} + \nu_{484} t^{484} + \nu_{485} t^{485} + \nu_{486} t^{486} + \nu_{487} t^{487} + \nu_{488} t^{488} + \nu_{489} t^{489} + \nu_{490} t^{490} + \nu_{491} t^{491} + \nu_{492} t^{492} + \nu_{493} t^{493} + \nu_{494} t^{494} + \nu_{495} t^{495} + \nu_{496} t^{496} + \nu_{497} t^{497} + \nu_{498} t^{498} + \nu_{499} t^{499} + \nu_{500} t^{500} + \nu_{501} t^{501} + \nu_{502} t^{502} + \nu_{503} t^{503} + \nu_{504} t^{504} + \nu_{505} t^{505} + \nu_{506} t^{506} + \nu_{507} t^{507} + \nu_{508} t^{508} + \nu_{509} t^{509} + \nu_{510} t^{510} + \nu_{511} t^{511} + \nu_{512} t^{512} + \nu_{513} t^{513} + \nu_{514} t^{514} + \nu_{515} t^{515} + \nu_{516} t^{516} + \nu_{517} t^{517} + \nu_{518} t^{518} + \nu_{519} t^{519} + \nu_{520} t^{520} + \nu_{521} t^{521} + \nu_{522} t^{522} + \nu_{523} t^{523} + \nu_{524} t^{524} + \nu_{525} t^{525} + \nu_{526} t^{526} + \nu_{527} t^{527} + \nu_{528} t^{528} + \nu_{529} t^{529} + \nu_{530} t^{530} + \nu_{531} t^{531} + \nu_{532} t^{532} + \nu_{533} t^{533} + \nu_{534} t^{534} + \nu_{535} t^{535} + \nu_{536} t^{536} + \nu_{537} t^{537} + \nu_{538} t^{538} + \nu_{539} t^{539} + \nu_{540} t^{540} + \nu_{541} t^{541} + \nu_{542} t^{542} + \nu_{543} t^{543} + \nu_{544} t^{544} + \nu_{545} t^{545} + \nu_{546} t^{546} + \nu_{547} t^{547} + \nu_{548} t^{548} + \nu_{549} t^{549} + \nu_{550} t^{550} + \nu_{551} t^{551} + \nu_{552} t^{552} + \nu_{553} t^{553} + \nu_{554} t^{554} + \nu_{555} t^{555} + \nu_{556} t^{556} + \nu_{557} t^{557} + \nu_{558} t^{558} + \nu_{559} t^{559} + \nu_{560} t^{560} + \nu_{561} t^{561} + \nu_{562} t^{562} + \nu_{563} t^{563} + \nu_{564} t^{564} + \nu_{565} t^{565} + \nu_{566} t^{566} + \nu_{567} t^{567} + \nu_{568} t^{568} + \nu_{569} t^{569} + \nu_{570} t^{570} + \nu_{571} t^{571} + \nu_{572} t^{572} + \nu_{573} t^{573} + \nu_{574} t^{574} + \nu_{575} t^{575} + \nu_{576} t^{576} + \nu_{577} t^{577} + \nu_{578} t^{578} + \nu_{579} t^{579} + \nu_{580} t^{580} + \nu_{581} t^{581} + \nu_{582} t^{582} + \nu_{583} t^{583} + \nu_{584} t^{584} + \nu_{585} t^{585} + \nu_{586} t^{586} + \nu_{587} t^{587} + \nu_{588} t^{588} + \nu_{589} t^{589} + \nu_{590} t^{590} + \nu_{591} t^{591} + \nu_{592} t^{592} + \nu_{593} t^{593} + \nu_{594} t^{594} + \nu_{595} t^{595} + \nu_{596} t^{596} + \nu_{597} t^{597} + \nu_{598} t^{598} + \nu_{599} t^{599} + \nu_{600} t^{600} + \nu_{601} t^{601} + \nu_{602} t^{602} + \nu_{603} t^{603} + \nu_{604} t^{604} + \nu_{605} t^{605} + \nu_{606} t^{606} + \nu_{607} t^{607} + \nu_{608} t^{608} + \nu_{609} t^{609} + \nu_{610} t^{610} + \nu_{611} t^{611} + \nu_{612} t^{612} + \nu_{613} t^{613} + \nu_{614} t^{614} + \nu_{615} t^{615} + \nu_{616} t^{616} + \nu_{617} t^{617} + \nu_{618} t^{618} + \nu_{619} t^{619} + \nu_{620} t^{620} + \nu_{621} t^{621} + \nu_{622} t^{622} + \nu_{623} t^{623} + \nu_{624} t^{624} + \nu_{625} t^{625} + \nu_{626} t^{626} + \nu_{627} t^{627} + \nu_{628} t^{628} + \nu_{629} t^{629} + \nu_{630} t^{630} + \nu_{631} t^{631} + \nu_{632} t^{632} + \nu_{633} t^{633} + \nu_{634} t^{634} + \nu_{635} t^{635} + \nu_{636} t^{636} + \nu_{637} t^{637} + \nu_{638} t^{638} + \nu_{639} t^{639} + \nu_{640} t^{640} + \nu_{641} t^{641} + \nu_{642} t^{642} + \nu_{643} t^{643} + \nu_{644} t^{644} + \nu_{645} t^{645} + \nu_{646} t^{646} + \nu_{647} t^{647} + \nu_{648} t^{648} + \nu_{649} t^{649} + \nu_{650} t^{650} + \nu_{651} t^{651} + \nu_{652} t^{652} + \nu_{653} t^{653} + \nu_{654} t^{654} + \nu_{655} t^{655} + \nu_{656} t^{656} + \nu_{657} t^{657} + \nu_{658} t^{658} + \nu_{659} t^{659} + \nu_{660} t^{660} + \nu_{661} t^{661} + \nu_{662} t^{662} + \nu_{663} t^{663} + \nu_{664} t^{664} + \nu_{665} t^{665} + \nu_{666} t^{666} + \nu_{667} t^{667} + \nu_{668} t^{668} + \nu_{669} t^{669} + \nu_{670} t^{670} + \nu_{671} t^{671} + \nu_{672} t^{672} + \nu_{673} t^{673} + \nu_{674} t^{674} + \nu_{675} t^{675} + \nu_{676} t^{676} + \nu_{677} t^{677} + \nu_{678} t^{678} + \nu_{679} t^{679} + \nu_{680} t^{680} + \nu_{681} t^{681} + \nu_{682} t^{682} + \nu_{683} t^{683} + \nu_{684} t^{684} + \nu_{685} t^{685} + \nu_{686} t^{686} + \nu_{687} t^{687} + \nu_{688} t^{688} + \nu_{689} t^{689} + \nu_{690} t^{690} + \nu_{691} t^{691} + \nu_{692} t^{692} + \nu_{693} t^{693} + \nu_{694} t^{694} + \nu_{695} t^{695} + \nu_{696} t^{696} + \nu_{697} t^{697} + \nu_{698} t^{698} + \nu_{699} t^{699} + \nu_{700} t^{700} + \nu_{701} t^{701} + \nu_{702} t^{702} + \nu_{703} t^{703} + \nu_{704} t^{704} + \nu_{705} t^{705} + \nu_{706} t^{706} + \nu_{707} t^{707} + \nu_{708} t^{708} + \nu_{709} t^{709} + \nu_{710} t^{710} + \nu_{711} t^{711} + \nu_{712} t^{712} + \nu_{713} t^{713} + \nu_{714} t^{714} + \nu_{715} t^{715} + \nu_{716} t^{716} + \nu_{717} t^{717} + \nu_{718} t^{718} + \nu_{719} t^{719} + \nu_{720} t^{720} + \nu_{721} t^{721} + \nu_{722} t^{722} + \nu_{723} t^{723} + \nu_{724} t^{724} + \nu_{725} t^{725} + \nu_{726} t^{726} + \nu_{727} t^{727} + \nu_{728} t^{728} + \nu_{729} t^{729} + \nu_{730} t^{730} + \nu_{731} t^{731} + \nu_{732} t^{732} + \nu_{733} t^{733} + \nu_{734} t^{734} + \nu_{735} t^{735} + \nu_{736} t^{736} + \nu_{737} t^{737} + \nu_{738} t^{738} + \nu_{739} t^{739} + \nu_{740} t^{740} + \nu_{741} t^{741} + \nu_{742} t^{742} + \nu_{743} t^{743} + \nu_{744} t^{744} + \nu_{745} t^{745} + \nu_{746} t^{746} + \nu_{747} t^{747} + \nu_{748} t^{748} + \nu_{749} t^{749} + \nu_{750} t^{750} + \nu_{751} t^{751} + \nu_{752} t^{752} + \nu_{753} t^{753} + \nu_{754} t^{754} + \nu_{755} t^{755} + \nu_{756} t^{756} + \nu_{757} t^{757} + \nu_{758} t^{758} + \nu_{759} t^{759} + \nu_{760} t^{760} + \nu_{761} t^{761} + \nu_{762} t^{762} + \nu_{763} t^{763} + \nu_{764} t^{764} + \nu_{765} t^{765} + \nu_{766} t^{766} + \nu_{767} t^{767} + \nu_{768} t^{768} + \nu_{769} t^{769} + \nu_{770} t^{770} + \nu_{771} t^{771} + \nu_{772} t^{772} + \nu_{773} t^{773} + \nu_{774} t^{7$$

any study of explicit corrections to the behavior of this quantity due to van der Waals forces. It is clear that these forces do not suffice to change the surface universality class. That is, the critical exponents will remain the same as in the case of completely short-range interactions [2, 19].

Let us now investigate in more detail the conditions under which the expansion in Eq. (1.1), leading to (1.2), can be justified. Some requirements, such as $2 < 0$, $(d+2) = 2 < 0$, are obvious and normally are satisfied in any realistic system for which $d = 3$ and 1 (i.e., for the 3d Ising model in which $\beta' = 0.034$ [21]). Important additional conditions arise, however, from the fact that we consider a finite system in which power law long-range surface fields (i.e. substrate-uid potentials) act. The influence of those long-range surface fields is felt everywhere in the finite system, the amplitude of the surface field being minimum at the center of the system. One can think of this smallest value as a type of a bulk field h , which has the effect of displacing the system from the position on the phase diagram on which its bulk field would otherwise place it. Taking into account contributions from both surfaces we obtain for the contribution of the long range surface field to an effective bulk symmetry-breaking field $h_{b;s} = 2h_{w;s} L = (2_0^+)$. Since the bulk magnetic field scales as $h[L=0^+] = 0$ one arrives at the criterion that in a finite system the finite-size contributions due to the long-range surface fields will be negligible in the critical region if

$$2h_{w;s} L = (2_0^+) \quad L = 0^+ = 1; \quad (1.8)$$

i.e.

$$2^{-1} h_{w;s} L = 0^+ = 1; \quad (1.9)$$

Note that $h_{w;s} > 0$ corresponds to attractive walls, i.e. walls preferring the liquid phase of the uid while $h_{w;s} < 0$ corresponds to repulsive walls, i.e. to walls preferring the gas phase of the uid. More detailed discussion on that point is presented in Appendix C, where we identify $h_{w;s}$ in the framework of a mean-field type model. Using the relations between critical exponents it is easy to show that $\beta = (d+2) = 2$. Thus the relation (1.9) is consistent with the form (1.1). On the other hand, $\beta = d = 3$ and, therefore, $\beta = d = 3$. By taking into account that for realistic systems $d = 3$, the condition (1.9) becomes

$$2^{-1} h_{w;s} L = 0^+ = 1; \quad (1.10)$$

For most systems 0^+ is of the order of 3 Å. Taking the values of β and β' to be appropriate to the 3d Ising model, we obtain in the case $\beta = 3$

$$L = L_{crit} + 2^{-1} h_{w;s} L = 612 h_{w;s}^{1/918} \text{ Å}; \quad (1.11)$$

Later on in this article we will discuss the determination of the magnitude of $h_{w;s}$ for the cases of ^3He and

^4He films bounded by Au surfaces. For the moment we note that in such systems $h_{w;s} \sim 10^{-4}$ (see Appendix C). The condition $L = 9000 \text{ Å}$ must be met if finite-size effects due to the van der Waals interactions are to be negligible within the critical region of an ^3He or ^4He film. If $L = 15000 \text{ Å}$, which is experimentally realizable, then one expects van der Waals finite-size effects to play an essential role everywhere within the critical region. This implies that the value of the finite-size susceptibility at T_c will depend on L and on the choice of the bounding substrate (i.e. on the value of $h_{w;s}$).

Away from T_c one expects

$$\chi = \chi_{bulk} + \frac{1}{L} \chi_{surface} + \frac{1}{L} \chi_{Hamaker} \quad (1.12)$$

In a uid system below T_c the Hamaker term comprises contributions due to both the uid-uid and the substrate-uid interaction (the substrate-substrate interaction does not contribute because the substrate density ρ_s does not depend on the magnetic field). In a uid system the density is the quantity that couples via the van der Waals type interaction. The average local density is non-zero both below and above the critical point, whereas in a magnetic system $m_0(T > T_c; H = 0) = 0$. Because of this, there exists a difference in the finite-size behavior of the uid and the magnetic systems when $T > T_c$. One can argue that for a magnetic system in which $T > T_c$ and $h = 0$ [26]

$$\chi = \chi_{bulk} + \frac{1}{L} \chi_{surface} + \frac{1}{L+1} \chi_{Hamaker} \quad (1.13)$$

Below T_c Eq. (1.12) is again valid. As we see, the terms of the order of $L^{-(d+1)}$ will never be important if substrate potentials are present in the system. Such terms, however, give rise to the leading finite-size contributions away from the critical region in the case of periodic boundary conditions [13, 14, 15, 18]. Contributions from the uid-uid potential are proportional to m^2 and, therefore, will be of importance only below the critical temperature (if $h \neq 0$). They then constitute one of the Hamaker terms.

Expressions similar to Eq. (1.2) have been shown to describe the finite-size behavior of the susceptibility in a fully finite system subject to periodic boundary conditions in which case $h_{w;s} = 0$ both in the instance of the exactly solvable spherical model [13, 14, 18] and via "expansion techniques (up to first order in ϵ)", in $O(n)$ models [15].

Figure 2 displays the behavior of the susceptibility in a film in which the interactions are completely short-range and of a film in which both the uid-uid and the uid-substrate interactions are long-range, the latter case corresponding to the actual experimental situation. We observe that the curves behave quantitatively differently in the two systems. At T_c and at coexistence, the susceptibility of the van der Waals type system is severely suppressed in comparison to that of the short-range system. As explained above and as we will see in more detail

below, the magnitude of the maximum depends on the strength of the substrate-uid coupling and is, therefore, not universal. Furthermore, there is a shift in the position of the maximum of the susceptibility. We expect that the curves shown here will resemble those obtained via experimental investigations.

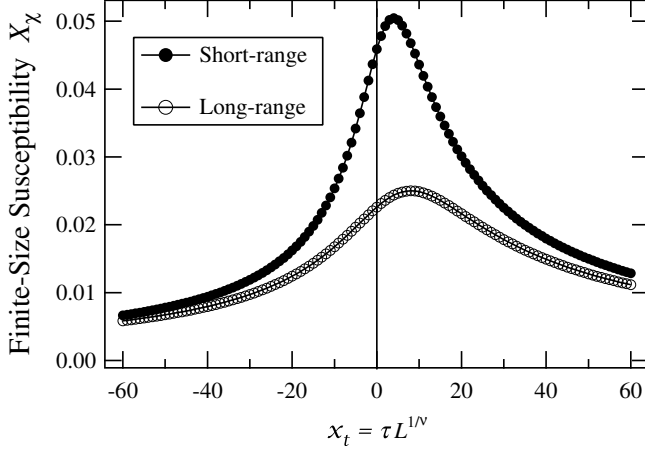


FIG. 2: A comparison between the behavior of the scaling functions of the susceptibility $X(x_t)$ for a uid in which both the substrate-uid and the uid-uid interactions are short-range and the same quantity for a uid in which both interactions are long-range. The thickness of the film is L_a , where $L = 3000$, while a is the average distance between the molecules of the uid. The scaling variable is $x_t = L^{1/\nu}$, where $\nu = 1/T_c - T$ with T_c being the critical temperature of the corresponding short- or long-range system. The curves differ essentially from each other, in that they have different magnitudes at T_c . The maximum of the scaled susceptibility is also shifted.

In this article, we will explore the mechanisms underlying the similarity of the susceptibility in a uid film near its bulk critical point to the susceptibilities plotted in Fig. 2. We investigate the behavior of the susceptibility as a function of the temperature, the external bulk magnetic field, the thickness of the film and the strength of the uid-substrate interaction.

The structure of the article is as follows. First, in Section II we present a precise formulation of the model of interest along with the analytical expressions needed for its numerical treatment. The principal results for the behavior of the finite-size susceptibility are presented in Section III. Some technical details [including sums containing van der Waals type potentials] can be found in Appendix A. An estimation of the parameters needed in order to apply the current results for the behavior of the susceptibility in ^3He and ^4He films is contained in Appendix C.

II. THE MODEL

Perhaps the simplest model that captures the basic features of systems with van der Waals interactions is a modification of the one utilized by Fisher and Nakanishi in their mean-field investigation of short-range systems [27, 28]. One starts with the following form of the functional for the free energy of the lattice system

$$F = \sum_r \left[\frac{1+m(r)}{2} \ln \frac{1+m(r)}{2} + \frac{1-m(r)}{2} \ln \frac{1-m(r)}{2} \right] - \sum_r h(r)m(r) - \frac{1}{2} \sum_{r,r^0} K(r;r^0)m(r)m(r^0); \quad (2.1)$$

where $K(r;r^0) = J^1(r;r^0)$ is the non-local coupling between magnetic degrees of freedom, $h(r)$ is an external magnetic field and the magnetization $m(r)$ is to be treated as a variational parameter. Note that in Eq. (2.1) the term in curly brackets corresponds to the entropic contributions, while the other terms are directly related to the interactions present in the system.

The variation of (2.1) with respect to $m(r)$ leads to the following equation of state for our system

$$m(r) = \tanh \left[\sum_{r^0} K(r;r^0)m(r^0) + h(r) \right]; \quad (2.2)$$

This equation can be solved numerically by applying the Newton-Kantorovich method. One is able to treat rea-

sonably thick films, with $L=a$ of the order of 3000 layers, corresponding to the experimental setup that we envisage as an example in our study. Its solution for a given geometry and external fields $h(r)$ determine the order-parameter profile $m(r)$ in the system.

We will be interested in a system with a film geometry. Then if $r = fr_k; zg$ and $h(r) = h(k; z) = h(z)$ one has, because of the symmetry of the system, $m(r) = m(k; z) = m(z)$. The magnetization profile now depends only on the coordinate perpendicular to the plates bounding the van der Waals system. In this case, Eq. (2.2), which describes the behavior of the magnetization profile,

becomes

$$m(z) = \tanh \sum_{r^0}^X J(r_k^0) m(z^0) + h(z); \quad (2.3)$$

where $r^0 = (r_k^0; z^0)$. Obviously, the above equation is equivalent to

$$m(z) = \tanh \sum_{z^0=0}^X \hat{J}(z-z^0) m(z^0) + h(z); \quad (2.4)$$

where

$$\hat{J}(z) = \sum_{r_k^0}^X J(r_k^0; z) = \sum_{r_k}^X J(r_k; z); \quad (2.5)$$

We will now assume that the fluid molecules occupy the region in space characterized by $0 \leq z \leq L$ and that the layers $z=0$ and $z=L$ satisfy the $(+; +)$ boundary conditions, i.e. $m(0) = m(L) = 1$. The number of layers containing spins that can fluctuate is, therefore, $L+1$.

Equation (2.4) is equivalent to

$$\operatorname{arctanh}[m(z)] = h(z) + \sum_{z^0}^X \hat{J}(z-z^0) m(z^0); \quad (2.6)$$

Taking the functional derivative of the both sides of Eq. (2.6) with respect to the field $h(z)$ applied to the layer z , we obtain

$$\frac{G(z; z)}{1 - m^2(z)} = \delta_{z;z} + \sum_{z^0}^X \hat{J}(z-z^0) G(z^0; z); \quad (2.7)$$

where

$$G(z; z) = \frac{m(z)}{h(z)} = \sum_{r_k}^X hS(0; z) S(r_k; z) i - hS(0; z) i hS(r_k; z) i; \quad (2.8)$$

Equation (2.7) can be rewritten in the form

$$\sum_{z^0}^X \frac{\delta_{z;z^0}}{1 - m^2(z^0)} \hat{J}(z-z^0) G(z^0; z) = \delta_{z;z}; \quad (2.9)$$

Now it is clear that the solution of the above equation with respect to $G(z^0; z)$ is

$$G(z^0; z) = R^{-1}_{z^0; z}; \quad (2.10)$$

where R^{-1} is the inverse matrix of the matrix R with elements

$$R_{z; z^0} = \frac{\delta_{z; z^0}}{1 - m^2(z^0)} \hat{J}(z-z^0); \quad (2.11)$$

One can define the "local" susceptibility

$$\chi(z) = \sum_{r_k}^X G(z; z) = \sum_{r_k}^X hS(0; z) S(r_k; z) i - hS(0; z) i hS(r_k; z) i; \quad (2.12)$$

Obviously, $\chi_z = (L+1)$ is the total susceptibility of the system per unit spin (see Eq. (2.12)). Thus, one has

$$\chi(z) = \sum_z^X R^{-1}_{z; z}; \quad (2.13)$$

and

$$\chi = \frac{1}{L+1} \sum_z^X R^{-1}_{z; z}; \quad (2.14)$$

In Appendix A we demonstrate that the function $\hat{J}(z)$ can be written in the form

$$\hat{J}(z) = J^1 \delta_{d-1}(z) + \delta_{d-1}^n [(z-1) + (z+1)] + G_d(z) \delta_{d-2}(z); \quad (2.15)$$

where $\delta(z)$ is the discrete delta function, while $\delta_{d-1}(z)$ is the Heaviside function. Explicitly for $d=3$ one has (see Appendix A)

$$c_2 = \sum_{n \geq 2}^X \frac{1}{1 + j^n j^n}, \quad 3.602; \quad (2.16)$$

$$c_2^{nn} = \frac{8}{3} \left((1)^{1=3} K_0 \left(\frac{1}{2 + 2i \frac{1}{3}} \right) - (1)^{3=3} K_0 \left(\frac{1}{2 + 2i \frac{1}{3}} \right) \right) + \frac{1}{3} \frac{1}{3} \ln 2 = 1.183; \quad (2.17)$$

and

$$G_3(x) = \frac{1}{3} \frac{1}{3} \arctan \frac{1}{2x^2} \ln \left(1 + \frac{1}{x^2} \right) + \frac{1}{2} \ln \left(1 + \frac{1}{x^2} + \frac{1}{x^4} \right); \quad (2.18)$$

The layer magnetic field $h(z)$ is the only quantity in Eq. (2.6) the exact form of which still requires specification.

We take it to be of the form

$$h(z) = \frac{h_{ws}}{(z+1)^3} + \frac{h_{ws}}{(L+1-z)^3}; \quad 1 \leq z \leq L+1; \quad (2.19)$$

where h_{ws} reflects the relative strength of the fluid-wall and fluid-fluid interactions (see Eq. (12) below). The above expression is consistent with the fact that the substrate occupies the region $R^{d-1} [L+1; 1] [R^{d-1} [(L+1); 1]]$. For ^3He and ^4He bounded by Au surfaces we show in Appendix C that $h_{ws} = 4$.

III. NUMERICAL RESULTS AND FINITE-SIZE SCALING ANALYSIS

To determine the total susceptibility $\chi(T; h, J; h_{ws})$ and its "scaling function"

$$\chi = L^{-\beta} \chi_m(z) \quad (3.1)$$

in a fluid film with thickness L , one has to solve Eq. (2.6) for $1 \leq z \leq L-1$, which allows one to construct the matrix R with the use of Eq. (2.11). Finally, on the basis of Eq. (2.13) one obtains the local susceptibility $\chi(z)$, $1 \leq z \leq L-1$, and, summing, the total susceptibility. We recall that within the mean-field treatment one has $\beta = 1/2$, $\gamma = 1$, $\nu = 0$ and, for the extraordinary surface transition, $\beta_s = 3/2$ [1].

The analytic solution to the set of coupled nonlinear equations for the magnetization profile is, at present, known only for purely short-range, continuous, systems [29]. We review this solution in section IIIA. Even in this case the finite-size susceptibility has to be determined numerically. The results are, again, presented in section IIIA. Numerical methods appear to be unavoidable in order to solve the equations for the magnetization profile in the case of the long-range interactions of the van der Waals type. The results in this case will be discussed in section IIIB.

A. The model with purely short-range interactions for $H = 0$

The equations to be solved in the continuum version of the purely short-range model of a mean-field Ising strip under $(+; +)$ boundary conditions are

$$1 = 1 - \frac{1}{c} \frac{\partial^2}{\partial z^2} + m^2(z) \chi(z); \quad (3.2)$$

$$0 = 1 - \frac{1}{c} \frac{\partial^2}{\partial z^2} + \frac{1}{3} m^2(z) \chi_m(z); \quad (3.3)$$

Because conditions are identical at both bounding surfaces of the system, the solutions of the above equation satisfy $m'(L/2) = 0$ and $\chi'(L/2) = 0$. The magnetization profile is known exactly [29]:

$$a) \text{ when } tL^2 \ll 2 \text{ [with } t = (T - T_c)/T_c]$$

$$\chi_m(z) = \frac{2K(k)}{L} \frac{\text{dn}(\cdot; k)}{\text{sn}(\cdot; k)}; \quad (3.4)$$

where

$$tL^2 = [2K(k)]^2 (2k^2 - 1); \quad \chi = [2K(k) = L] z; \quad (3.5)$$

and $k^2 \geq 0$.

$$b) \text{ when } tL^2 \gg 2$$

$$\chi_m(z) = \frac{2K(k)}{L} \frac{1}{\text{sn}(\cdot; k)}; \quad (3.6)$$

where

$$tL^2 = [2K(k)]^2 (k^2 + 1); \quad \chi = [2K(k) = L] z; \quad (3.7)$$

and $k^2 \geq 0$.

Here $K(k)$ is the complete elliptic integral of the first kind, $\text{dn}(\cdot; k)$ and $\text{sn}(\cdot; k)$ are the Jacobian amplitude and the sine amplitude functions, respectively. The bulk critical point $T = T_c$ corresponds to $k^2 = 1/2$. The above expressions are consistent with the following scaling form for the order parameter:

$$\chi_m(z) = L^{-\beta} \chi_m\left(\frac{z}{L}; tL^{1-\nu}\right); \quad (3.8)$$

with $\beta = 1/2$.

The results from the finite-size scaling analysis of the behavior of the susceptibility for a system with short-range interactions are summarized in Figs. 3 and 4. Fig. 3 compares the finite-size susceptibilities $\chi_m = \chi(T; h, J; h_{ws})$ for short-range films with $L = 100$ and $L = 3000$ layers. Fig. 4 presents the corresponding results for the ratio $\chi(T; h, J; h_{ws} = 0) / \chi(T = T_c; h = 0, J; h_{ws} = 0)$. In both plots the scaling variable is $x_t = (1 - T_c/T)L^{1-\nu}$. The curves demonstrate a reasonably good scaling where the small deviations for $L = 100$ from the $L = 3000$ curve can be explained with the ambiguity in the definition of L (for a discussion see Appendix B), as well as with the corrections to scaling terms and the role of the background (nonuniversal terms). Note that the curves present the behavior of the total susceptibility and not only of its singular part.

B. The model with van der Waals type interactions

We note that the critical temperature T_c depends on the presence or absence of long-range fluid-fluid interactions in the system. Let us denote by $T_{c;lr}$ the critical temperature of the system with subleading long-range fluid-fluid interactions (from van der Waals type) and with $T_{c;sr}$ the corresponding temperature for short-range fluid-fluid interactions. If $K = 1/2$ then it is straightforward to show that $K_{c;lr}' \approx 0.161$, while $K_{c;sr}' \approx 0.168$ in the framework of our model defined by Eq. (1).

The results from the finite-size scaling analysis of the behavior of the susceptibility for a system with long-range van der Waals type interactions are presented in Figs. 5, 6, 7, 8, 9 and 10. The scaling procedure is explained in details in Appendix B.

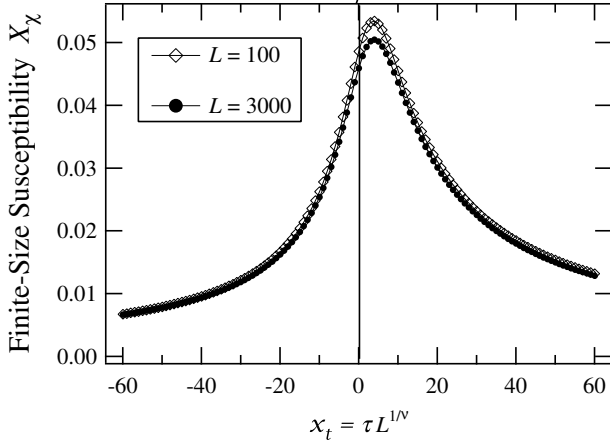


FIG. 3: The upper dotted line, for $L = 100$, and the lower dotted line, for $L = 3000$, illustrate the behavior of the scaling function of the susceptibility $X_\chi(x_t)$ for a uid in which both the substrate-uid and the uid-uid interactions are short-range. The scaling variable is $x_t = (1 - T_c/T)L^{1/\nu}$. Note that the maximum of the finite-size curves is at $T > T_c$ which is due to the stabilizing effect of the $(+; +)$ boundary conditions on the order parameter in the finite system. We observe that the both curves differ at most around their maximal value. As it will be demonstrated in Fig. 4 the principal reason for this deviation is the improper choice of the value of the distance L between the plates.

1. The temperature dependence at $H = 0$

Let us first consider the behavior of the finite-size susceptibility in the absence of an external magnetic field, which is equivalent to the behavior in a uid system along the liquid-vapor coexistence line. Our results are presented in Figs. 5 and 6. One observes that the susceptibility possesses a maximum above the bulk critical temperature (which reflects that fact that the $(+; +)$ boundary condition stabilize the long-range order at temperatures slightly above T_c) and that this maximum is weaker than for the corresponding short-range system (see Fig. (3)). The scaling variable is $x_t = (1 - T_c/T)L^{1/\nu}$. Note that the scaling functions decay much more slowly as a function of $|x_t|$ in comparison with the short-range case. The maximum of the short-range case is around $x_t \approx 4$ while in the case of a van der Waals type system it is around $x_t \approx 8$. These results imply that, as expected, the long-range tails of the interactions help to stabilize the long-range order even a bit above the corresponding limit in T for the short-range system with $(+; +)$ boundary conditions.

2. The temperature dependence of the susceptibility at $H \neq 0$

In this section we consider the behavior of the finite-size susceptibility for values of the external bulk magnetic

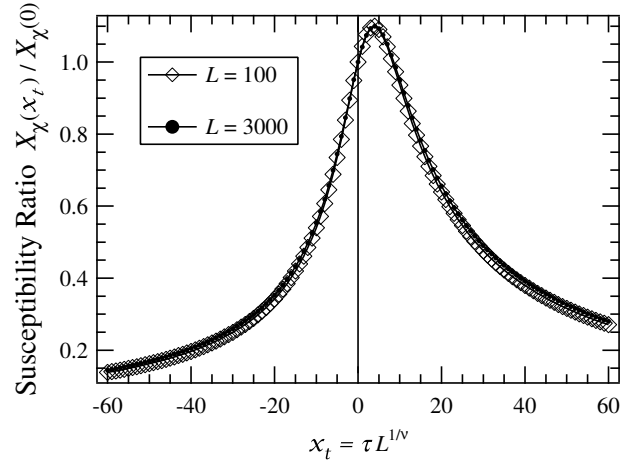


FIG. 4: The lines show the behavior of the scaling function of the normalized susceptibility $X_\chi(x_t) = X_\chi(0)$ for a uid in which both the substrate-uid and the uid-uid interactions are short-range. The curves are for $L = 100$ and for $L = 3000$. The scaling variable is $x_t = (1 - T_c/T)L^{1/\nu}$. Both curves coincide perfectly well with each other. The main reason for the deviation of the curves in Fig. 3 is the improper choice of the length L (for a discussion see Appendix B).

field that support the vapour phase of the uid. The results are presented in Fig. 7. Note that by changing the sign of H (by choosing negative values of $x_h = H L^\nu$) one can show that the position of the maximum in the behavior of the susceptibility, which for $H = 0$ is at $T > T_c$, moves gradually toward T_c and for negative field with large enough magnitude can even be below T_c . In Fig. 8 we present the above results as a function of $L = t$. This resolves the question about the value of the nonuniversal metric factor in x_t . Note that then the shape of the curve and the position of its maximum shall be a reasonable approximation for the real experimental system of ^3He or ^4He films bounded by Au surfaces.

3. The field dependence of the susceptibility at $T \neq T_c$

Here we analyze the behavior of the finite-size susceptibility as a function of the field scaling variable $x_h = H L^\nu$ for fixed values of the temperature close to the bulk critical temperature T_c . The results are presented in Fig. 9. The curves are for $\beta = 0; 10^{-6}; 10^{-5}; 10^{-4}$. Note that the behavior of the susceptibility possesses a peak that essentially differs from the corresponding background contribution only for $\beta \geq 10^{-6}$. In Fig. 10 we present the same results, this time as a function of $L = h$. This resolves the question about the value of the possible nonuniversal metric factor in x_h . Thus, the shape of the curve and the position of its maximum shall be a reasonable approximation for the real experimental system of ^3He or ^4He films bounded by Au surfaces.

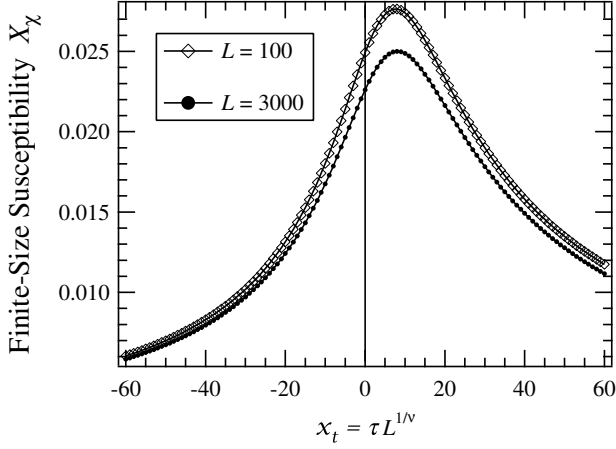


FIG. 5: The upper dot line (for $L = 100$) and the lower dot line for ($L = 3000$) show the behavior of the scaling function of the susceptibility $X_\chi(x_t)$ for a uid in which both the substrate-uid and the uid-uid interactions are of van der Waals type, i.e. are long-range. The scaling variable is $x_t = (1 - T_c/T)L^{1/\nu}$. We observe that both curves differ at most around their maximal value. The amplitude of the surface eld for $L = 100$ is $h_{w,js} = 0.73$ while for $L = 3000$ it is $h_{w,js} = 4$ which ensures that the variable $2^{s+1}h_{w,js}[L=0]^+ = 2^{4.5}h_{w,js}[L=0]^+ = 2$ has the same value for both the cases.

IV. CONCLUDING REMARKS AND DISCUSSION

In this article we investigated the behavior of the susceptibility in thin films with van der Waals type long-range interactions. Prominent examples of such systems are simple nonpolar uids in thermodynamic equilibrium with their vapor, as well as binary uid mixtures close to their demixing point. We have seen that despite the fact that this kind of interaction does not change the critical exponents of the system it nevertheless gives rise to a variety of finite-size effects that become dominant when $L = 1$. Furthermore, we have formulated a criterion regarding the conditions under which such effects also essentially modify the finite-size behavior of the susceptibility everywhere within the critical region. According to this criterion if the thickness L of the film is such that (see Eq. (1.11))

$$L > L_{\text{crit}} = \frac{1}{h_{w,js}^2} (16h_{w,js})^+; \quad (4.1)$$

the effects due to the van der Waals interaction are essential and cannot be neglected. Here $h_{w,js}^+$ is the amplitude of the bulk correlation length while the (dimensionless) factor $h_{w,js}$ characterizes the strength of the uid-substrate interaction $h_{w,js}z$, where z is the distance from the substrate surface toward to the bulk of the uid. In the case of ^3He or ^4He bounded by Au surfaces we find that at the corresponding critical point of both the uids $h_{w,js} \approx 4$ (see Appendix C). Then, for a three-dimensional Ising type system the direct evalu-

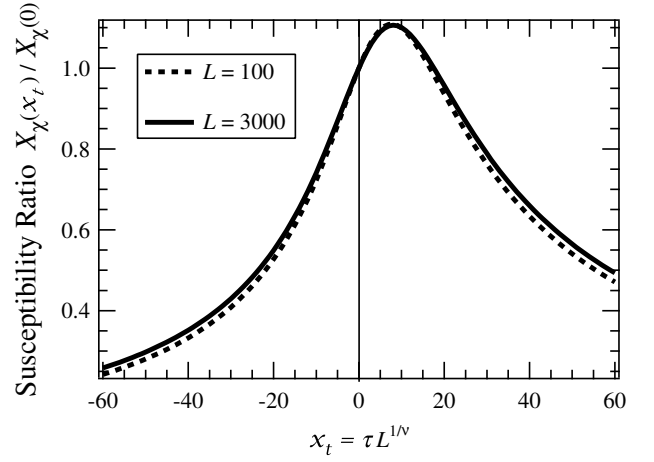


FIG. 6: The lines show the behavior of the scaling function of the normalized susceptibility $X_\chi(x_t)/X_\chi(0)$ for a uid in which both the substrate-uid and the uid-uid interactions are long-range. The curves are for $L = 100$ and for $L = 3000$. The scaling variable is $x_t = (1 - T_c/T)L^{1/\nu}$. We observe that the both curves coincide perfectly well with each other only near the bulk critical point. The deviation of the curves from each other is due to the effect of the van der Waals interaction (compare with the short-range case) and increases with the increase of $|x_t|$. Note also that the scaling function decays much slower with $|x_t|$ in comparison with the short-range case.

ation yields the estimate $L_{\text{crit}} \approx 9000 \text{ \AA}$. A comparison when $L = a = 3000$ layers (where a is the lattice constant) between the behavior of the finite-size susceptibility of a system with completely short-range interactions and one with long-range uid-uid and substrate-uid interactions is given in Fig. 2. One observes a clear distinction between the curves in the critical region. The calculations were performed using a mean-field type model which is described in detail in Section II. In order to determine the susceptibility one solves $L = a = 3000$ coupled nonlinear equations; we make use of the Newton-Kantorovich method. We have chosen a film with this number of layers because it corresponds to a realistic experimental setup of ^3He film between the Au electrodes of an experimental cell in which the smallest distance between the plates is 1.5 \mu m ; the distance r_0 between the atoms of ^3He at its liquid-vapor critical point has been estimated to be $r_0 \approx 4.9 \text{ \AA}$ (see Appendix C). For such a system the behavior of the susceptibility as a function of $(1 - T_c/T)L^{1/\nu}$ for different values of the bulk eld $x_h = H/L^\nu$ is shown in Fig. 7, while in Fig. 9 the susceptibility is plotted as a function of x_h for a few fixed values of t . The same data are shown in Figs. 8 and 10 as functions of $L = t$ and $L = h$, respectively. We expect these curves to resemble the actual experimental data for ^3He (or ^4He) film. One observes that for $x_h = 0$, the maximum of the susceptibility is above the bulk critical point. Furthermore, we note that when one is on the vapor side of the bulk phase diagram the maximum

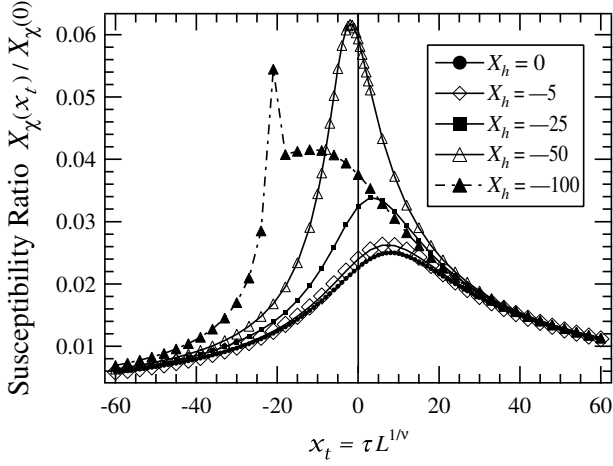


FIG. 7: The lines show the behavior of the scaling function of the susceptibility $X_\chi(x_t; x_h)$ for a fluid in which both the substrate-fluid and the fluid-fluid interactions are long-range. The substrate-fluid potential is characterized by $h_{ws} = 4$, which correspond to the situation of ^3He or ^4He in bounded by Au surfaces (see Appendix C). The curves are for $L = 3000$ and at $x_h = 0; 5; 25; 50; 100$, where $x_h = H L^{-1/3}$. The scaling variable is $x_t = (1 - T_c/T) L^{1/3}$. The changed shape of the curve for $x_h = -100$ signals that this curve is the precursor of a first-order phase transition.

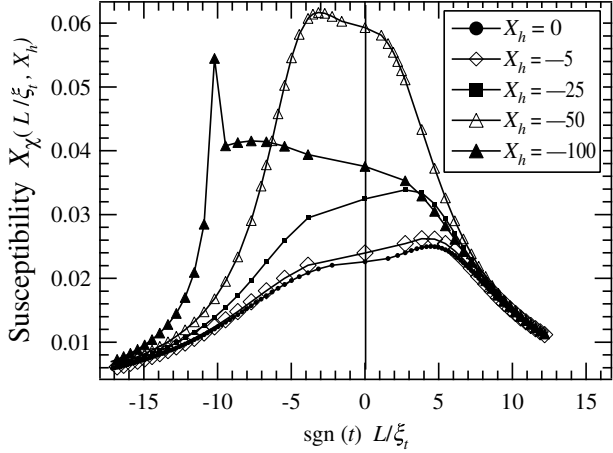


FIG. 8: The same as in Fig. 7 but the scaling function is presented as a function of $L = L_t$ at several fixed values of x_h . We expect this curve to be a good approximation of the corresponding finite-size scaling function for a real three-dimensional experimental system of ^3He or ^4He in bounded by Au surfaces.

moves toward the bulk critical point with increasing distance from the coexistence curve in the phase diagram as a function of x_h and that for x_h large enough the maximum positions itself at a temperature less than T_c . Additionally, one observes that as a function of the scaling field variable (x_h , or $y_h = L = x_h^{-3}$) the susceptibility does not display an easily distinguishable maximum unless $|x_h| > 10^{-6}$. The position of this maximum changes

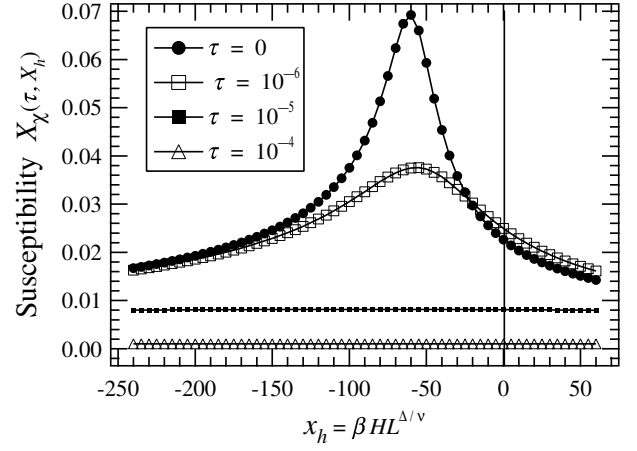


FIG. 9: The lines show the behavior of the scaling function of the susceptibility $X_\chi(x_t; x_h)$ as a function of x_h at several fixed values of x_t for a fluid in which both the substrate-fluid and the fluid-fluid interactions are long-range. The substrate-fluid potential is characterized by $h_{ws} = 4$, which correspond to the situation of ^3He or ^4He in bounded by Au surfaces (see Appendix C). The scaling variable is $x_h = H L^{-1/3}$. The numerical calculations are performed for $L = 3000$ layers.

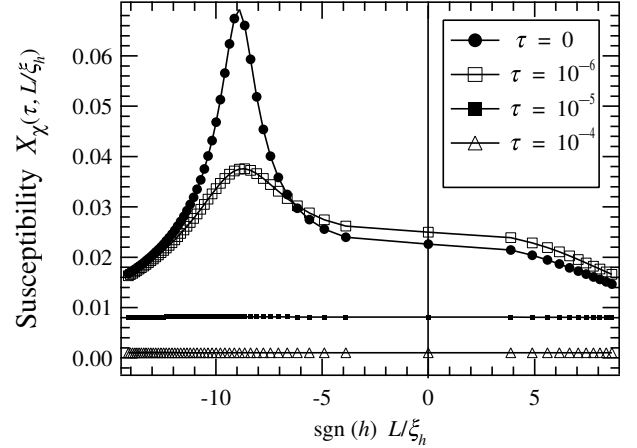


FIG. 10: The same as in Fig. 9 but the scaling function is presented as a function of $L = L_h$ at several fixed values of τ . We expect this curve to be a good approximation of the corresponding finite-size scaling function for a real three-dimensional experimental system of ^3He or ^4He in bounded by Au surfaces.

very slightly with t and is around $\text{sign}(h)L = x_h^{-3}$ on the vapor side of the bulk phase diagram.

We stress that all of the above curves depend on the value of h_{ws} and are, thus, nonuniversal. This implies that if h_{ws} is kept fixed when L changes one will obtain different curves for the different L 's. The same will also be true when L is kept fixed but h_{ws} changes. This is illustrated in Appendix B | see Figs. 12 and 13. Only when $h_{ws} = L$ is kept fixed can a curve that does not depend on L nor on h_{ws} , but just on their ratio, be ob-

tained – see Fig. 14. In practice, one does not know the precise value of the system size L – an important issue for very thin film thicknesses (for more details see Appendix B). When this is also taken into account further improvement of the data collapse can be achieved as seen in Fig. 15, where the corresponding data for the susceptibility for fixed $h_{w,s} = L$ are normalized by its value at the bulk critical point. Definitely the above predictions are clearly experimentally verifiable. For a given fluid, one can either change the size L of the distance between the plates of the experimental cell (i.e. the fluid film) or the corresponding substrate (i.e. the value of $h_{w,s}$). The bigger the change in the new $h_{w,s}$, the bigger will be the deviation of the new curve of the finite-size susceptibility from the old one. Of course, this will be possible only if $L \neq L_{crit}$. When $L = L_{crit}$ the universal behavior of the finite-size susceptibility in its standard form will prevail and the van der Waals interaction will only lead to small, probably experimentally negligible, corrections to the universal curve. Let us also note that when the experiment is performed for ^3He or ^4He around their liquid-vapor critical points according to our predictions one will obtain for any fixed L (even when $L = L_{crit}$) (practically the same curve X for the finite-size susceptibility of both the fluids. For $L = L_{crit}$ this will be simply due to the fact that $h_{w,s} \sim 4$ for both the fluids (see Appendix C), while for $L \neq L_{crit}$ that will be due to universality since near their liquid vapor critical points these fluids belong to the three-dimensional Ising universality class.

In the work described above, the effects of retardation on the van der Waals force have been neglected. These effects set in for distances r larger than 160 \AA between the He and Au atoms [30]. A possible concern is the influence of retardation on the system investigated in this paper. We have estimated that influence by performing numerical calculations in which an "extreme" retardation was imposed, in that the interaction potential was set to zero for separations $r > 100$ layers. We discovered that the numerical consequence of retardation grows with increasing film thickness. At $L = 3000$ the difference between the calculation with the unretarded van der Waals force and the force with long-distance cutoff is 13.5% at $T = T_c$. This is an overestimate of the actual influence of retardation in experimental realizations. We note that retardation reduces the suppression of the susceptibility by the van der Waals interaction – see Fig. 2.

Finally, let us note that in the current study we did not take into account the influence of gravity on the behavior of the finite-size susceptibility. Because gravity leads to stratification of the density one expects an additional, more complicated z dependence of the local and, therefore, of the total susceptibility. We hope to return to this

question in a future publication.

Acknowledgments

A portion of this work was carried out under a contract with the National Aeronautics and Space Administration.

DD acknowledges the partial financial support under grant F-1402 of the Bulgarian NSF.

APPENDIX A: DERIVATION OF THE EQUATION FOR THE MAGNETIZATION PROFILE IN A VAN DER WAALS FILM

Here we derive an explicit form for the function $\hat{J}(z)$ for some basic cases of special physical interest. Namely we take $J(r)$ to be of the "van der Waals form"

$$J(r) = \frac{J}{1 + r^{d+}}; \quad (\text{A } 1)$$

where $r = |\mathbf{r}|$, and $d = 3$ for the "real" (nonretarded) van der Waals interaction.

Then one can further simplify the sum in the right-hand side of the above equation. Using the identity

$$\frac{1}{1+z} = \sum_{k=0}^{\infty} (-z)^k \exp(-zt) t^{k-1} E_1(-t); \quad (\text{A } 2)$$

where

$$E_1(z) = \sum_{k=0}^{\infty} \frac{z^k}{(k+1)!}; \quad z > 0; \quad (\text{A } 3)$$

are the Mittag-Leffler functions, the sum can be rewritten in the form

$$\sum_{r^0}^X J(r^0) m(z^0) = \sum_{z^0=0}^X \hat{J}_{d;}(z^0) m(z^0); \quad (\text{A } 4)$$

where

$$\begin{aligned} \hat{J}_{d;}(z) &= \sum_{k=0}^X \int_0^{\infty} dt t^{(d+)=2-1} E_{\frac{d+}{2}, \frac{d+}{2}}(-t^{(d+)=2}) \\ &\otimes \sum_{r_k}^X e^{tr_k^2 A} e^{-tz^2}; \end{aligned} \quad (\text{A } 5)$$

The main advantage of the above form is that it factorizes the summation over the components of r_k^0 . With the help of the Poisson identity Eq. (A 4) becomes

$$\begin{aligned}
X_{r^0} J(r^0 m(z^0)) &= J^0 \sum_{r_k^0} \frac{1}{1+r_k^{d+}} A_m(z) \\
&+ J \int_0^1 dt \frac{1}{t} t^{(d-1)/2-1} E_{\frac{d+}{2}, \frac{d+}{2}} \left(\frac{t^{d+}}{t^2} \right) X^L e^{t(z-z^0)^2} m(z^0) \\
&+ J \int_0^1 dt \frac{1}{t} t^{(d-1)/2-1} E_{\frac{d+}{2}, \frac{d+}{2}} \left(\frac{t^{d+}}{t^2} \right) X^L e^{t^2 n^2} X^L e^{t(z-z^0)^2} m(z^0);
\end{aligned} \quad (A 6)$$

where n^2 is a $(d-1)$ -dimensional vector with integer components, and all the lengths are measured in units of lattice spacings. It is easy to show that $\max_t \exp(-n^2 t + t(z-z^0)^2)$ is attained at $t = \frac{1}{2n^2}$ and is equal to $\exp(-\frac{1}{2n^2})$. Because of this exponential decay in the last row of the above equation we will take into account only the terms with $j=1$ and $j=2$ (the corresponding improvements that take into account $n=2;3$ and $j=2;3$ are obvious; as we will see even the contributions stemming from $j=1$ and $j=2$ are very small). It is clear that size dependent contributions that are due to the terms in the last row of (A 6) will be exponentially small in L .

For $d=3$ the corresponding Mittag-Leffler function can be expressed in the following simple form

$$E_{3,3}(t^3) = \frac{1}{3t^2} e^{-t} - 2e^{-t} \cos \frac{p\sqrt{3}}{3} t + \frac{p\sqrt{3}}{2} t^2 \quad (A 7)$$

Taking into account that, if $x > 0$,

$$\int_0^1 dt E_{3,3}(t^3) e^{-tx} = G_3(x); \quad (A 8)$$

where

$$\begin{aligned}
G_3(x) &= \frac{1}{3} \frac{p\sqrt{3}}{3} \arctan \frac{p\sqrt{3}}{2x-1} - \ln \left(1 + \frac{1}{x} \right) \\
&+ \frac{1}{2} \ln \left(1 + \frac{1}{x} + \frac{1}{x^2} \right); \quad (A 9)
\end{aligned}$$

we arrive at the following equation for the magnetization profile

$$\begin{aligned}
\operatorname{arctanh}[m(z)] &= h(z) + K \sum_{j=2}^8 c_2 m(z) + c_2^{nn} [m(z+1) + m(z-1)] + \sum_{j=2}^9 G_3(j^2 z^0) m(z^0); \quad (A 10)
\end{aligned}$$

where

$$c_2 = \sum_{n^2 \geq 2} \frac{1}{1+n^2}, \quad 3.602; \quad (A 11)$$

and

$$\begin{aligned}
c_2^{nn} &= \frac{8}{3} \int_0^1 dt e^{-t^2} \cos \frac{p\sqrt{3}}{2} t + \frac{p\sqrt{3}}{3} + G_3(1) \\
&= \frac{8}{3} \left((1)^{1/3} K_0 \left(\frac{p\sqrt{3}}{2} \right) + \frac{p\sqrt{3}}{3} \right) \\
&\quad + \frac{8}{3} \left((1)^{2/3} K_0 \left(\frac{p\sqrt{3}}{2} \right) + \frac{p\sqrt{3}}{3} \right) \ln 2 \\
&\approx 0.00955 + 1.17354 - 1.183; \quad (A 12)
\end{aligned}$$

As we see, the contribution due to the first part in Eq. (A 12), and therefore the contributions due to the last row of Eq. (A 6) are of the order of 1% in the constant c_2^{nn} . It is easy to verify that

$$G(x) \approx \frac{1}{2} x^{-2} - \frac{1}{5} x^{-5} + \frac{1}{8} x^{-8} + O(x^{-11}); \quad x \gg 1; \quad (A 13)$$

Setting $G=0$ in Eq. (A 10) one obtains an equation having a form that is familiar in the mean-field theory of short-range systems. Actually in our case the system in question has short-range interactions in z direction and long-range ones within the planes perpendicular to z . The standard Ginzburg-Landau equation follows, for small m , after taking into account that $\operatorname{arctanh}(m) \approx m + m^3/3 + O(m^5)$. A continuum version of the equation

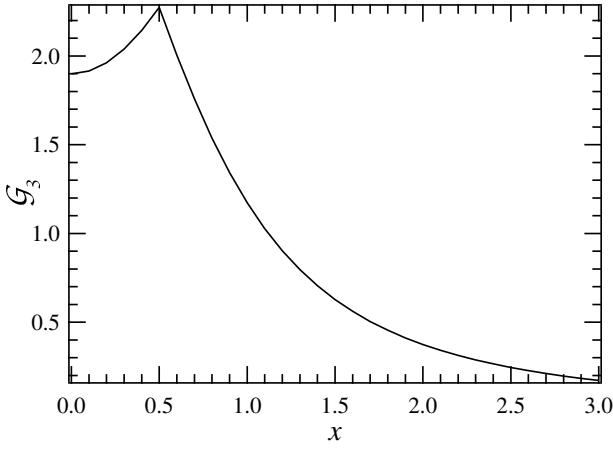


FIG. 11: The behavior of the G_3 -function as defined in (A.9).

follows from the replacement $m(z-1) + m(z+1) \rightarrow 2m(z) + m''[z]$. Obviously such a continuum version can also be constructed for the long-range system by adding the terms contributed by the function $G(x)$, which is, in this case, a continuous function. Note that the function $G(x)$ is well defined everywhere for $x \geq 0$ and not only for $x \geq 1$ as we actually need it in the lattice formulation of the theory. Thus, in the continuum formulation of the theory the integration can be extended over the region $z \in [0; L]$. This does not change the long-range behavior of the magnetization profiles. In the continuum case the equation for the magnetization profile reads

$$m[z] + \frac{1}{3}(m[z])^3 = h[z] + K \left(c_2 m[z] + c_2^{nn} 2m[z] + \frac{d^2 m[z]}{dz^2} + \int_0^z G(z-z') m(z') dz' \right) : \quad (\text{A.14})$$

APPENDIX B: HOW TO SCALE

In the discussion up to now we have tacitly assumed that the value of L is precisely known. This is, however, not only an experimental problem [due to the roughness of the surface, the existence of impurities, dust, etc.] but also a theoretical problem that might play a role when L is not "large enough". Let us make a brief comment about this issue. The definition of the size of the system is unambiguous only for systems with periodic boundary conditions. If N is the number of layers with independent degrees of freedom, then the size of the system is simply $L = Na$, where a is the distance between the layers. Any point in the system is equivalent to any other point. Therefore, any layer is equally suitable to be taken as the origin with respect to which one measures distance. However, how one proceeds for a system with $(+; +)$ boundary conditions [when the first and the last layers have fixed degrees of freedom] is less clear. For consistency with periodic boundary conditions one can, of course, count the number of layers with independent degrees of freedom and let this, as in the case of periodic boundary conditions, be equal to N . Then the question is, shall we include in the total size of the system the half distance between the two outermost layers with independent degrees of freedom and the adjacent layers with the fixed degrees of freedom? A reasonable approach seems to be that at least half of these distances should be taken to belong to the system, i.e. $L = (N+1)a$. This, of course, is not an unambiguous procedure. We have two layers

with fixed degrees of freedom, which do not belong to the "substrate" surrounding the system that strongly prefers the ordered phase of the system in the case of $(+; +)$ boundary conditions. Thus one has to somehow decide which portion of the bounding layers are to be counted within the system. Much more complicated is the case of systems with long-range interactions. Then any particle (atom, or molecule) of the system interacts with any other one from the substrate. How then does one define the size of the system or the borderline between the substrate and the system? Let us denote by \hat{L} the "true" size of the system (which we do not know), and by L a reasonable approximation of that size (say, by taking, as above for the short-range case, the size to be $L = (N+1)a$). The last implies that $\hat{L} = L + \delta$, where $\delta \ll \hat{L}$. Figure 12 demonstrates the difficulties when studying the scaling in systems with subleading long-range interactions of the van der Waals type. The role of the long-range surface potentials, which are irrelevant in the renormalization group sense but for moderate values of L , i.e. for $a \ll L \ll L_{\text{crit}}$ (see Eq. (1.11)), contribute to the leading behavior of the finite-size susceptibility is clearly seen. One can say that, for such values of L , the quantity x_s is a sort of "dangerous" irrelevant variable in the sense that, despite being irrelevant, one cannot neglect it when $L < L_{\text{crit}}$. We further note that the greatest deviation of the curves for different L from each other is around the maximum value of the scaling functions. The lack of the data collapse is due to the fact that $x_{w;s} = \frac{L}{L_{\text{crit}}}$ is not the same for all the curves (see Eq. (1.11)). Definitely

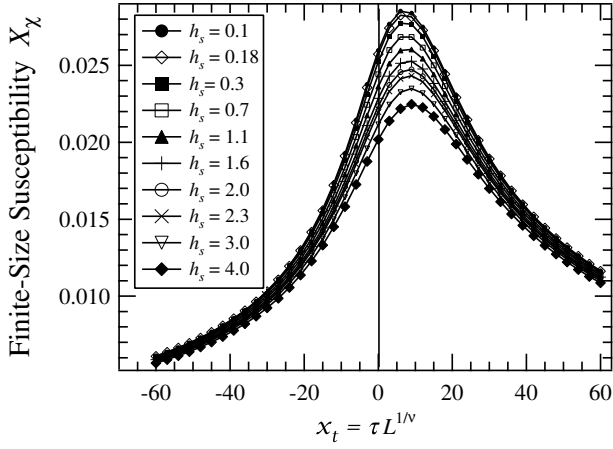


FIG. 12: The behavior of the finite-size susceptibility normalized per $L^{-\beta}$ for different fixed values of $h_{w,s}$ and for $L = 500$. Within the mean-field approximation one has that $\beta = 3$. The values of $h_{w,s}$ for which results are presented are $h_{w,s} = 0.1; 0.18; 0.3; 0.7; 1.1; 1.6; 2.0; 2.3; 3.0$ and 4.0 . They model the role of different substrates that surround a given fluid film with thickness L .

similar spreading of the data for the finite-size susceptibility are to be observed if $h_{w,s}$ is kept fixed while L changes (say $h_{w,s} = 4$ as in case of ^3He or ^4He confined by Au plates and one considers $L = 3000; 1000; 500; 100$ (see Fig. 13). However, when x_s is kept fixed for the

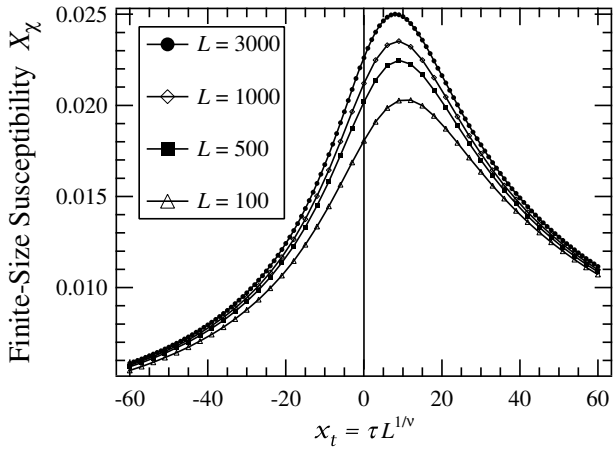


FIG. 13: The behavior of the finite-size susceptibility normalized per $L^{-\beta}$ for different fixed values of L with the surface-field amplitude kept fixed at $h_{w,s} = 4$. Systems with thickness $L = 3000; 1000; 500$ and $L = 100$ are considered. The curves represent the behavior of the susceptibility of ^3He and ^4He films with different thickness when the surrounding surfaces are made of gold.

same values of L considered before, the data collapse improves greatly, as shown in Fig. 14. One observes that violations of scaling are now clearly detectable only for the smallest system size $L = 100$. Let us now recall that

when L is "large but small enough" the effect of ϵ , i.e. of the fact that we do not know exactly the system size L is clearly evident. In the case of one has $\hat{L} = [L + \epsilon] = \hat{L}^1 + O(\hat{L}^{-2})$ [X($\hat{x}_t; \hat{x}_h; \hat{x}_s; \hat{x}_b; \hat{x}_l$)], where $\hat{x}_t = a_t \hat{L}^{1-\epsilon}$, $\hat{x}_h = a_h h \hat{L}^{-\epsilon}$, $\hat{x}_s = h_{w,s} \hat{L}^{(d+2-\epsilon)/2}$, $\hat{x}_b = b \hat{L}^{2-\epsilon}$, $\hat{x}_l = a_l \hat{L}^{1-\epsilon}$. Note now that the expansion of the above expressions in terms of \hat{L} will yield all possible non-universal (proportional to \hat{L}^{-1}) corrections to the leading finite-size behavior of the susceptibility with the greatest deviation of the curves for different L occurring near the maximum value of X . For the sake of precision let us also note that similar corrections will be produced if one takes into account the change from L to \hat{L} in the variables $\hat{x}_t; \hat{x}_h; \hat{x}_s; \hat{x}_b$ and \hat{x}_l . Thus, only the leading finite-size behavior can be determined unambiguously. All corrections will depend on the definition of L , i.e. on ϵ . There is, nevertheless, still something that one can do in order to check that the behavior of the susceptibility for $L = 100$ is simply due to the above explained unambiguity in the definition of L . Note, that if we normalize X to its value at a given point within the critical region (say to the value X_0 at the bulk critical point ($T = T_c, H = 0$)) then, whatever the definition of L is, the leading behavior of the resulting quantity will not depend on this definition. Explicitly, we have

$$\frac{X(\hat{x}_t; \hat{x}_h; \hat{x}_s; \hat{x}_b; \hat{x}_l)}{X_0} = \frac{X(\hat{x}_t; \hat{x}_h; \hat{x}_s; \hat{x}_b; \hat{x}_l)}{X(0; 0; \hat{x}_s; \hat{x}_b; \hat{x}_l)} + O(\hat{L}^{-1}). \quad (B1)$$

The result from the application of the above procedure is

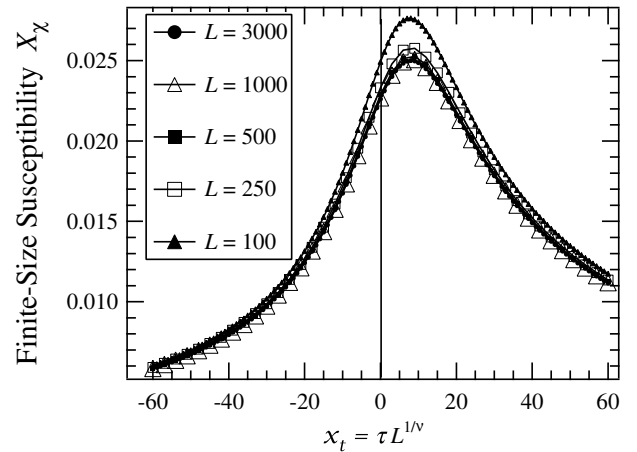


FIG. 14: The finite-size susceptibility for $L = 3000, L = 1000, L = 500, L = 250, L = 100$. The amplitude of the surface magnetic field is rescaled in such a way that $h_{w,s} = \bar{L} = \text{const}$ for all values of L and, as in the experimental realization, $h_{w,s} = 4$ for $L = 3000$. One observes that practically all the curves for $L \geq 250$ coincide with each other, i.e. the scaling is indeed valid. The curve with $L = 100$ differs from the others. Thus $L = 100$ is too small, and in this case the importance of ϵ is demonstrated.

shown in Fig. 15. We observe that all the curves, including $L = 100$, now allow for data collapse and that only a

small deviation of the curves from each other is observed for very large values of the scaling variable x_t , when the onset of the nonuniversal corrections to scaling due to the role of the uid-uid interaction (i.e. proportional to x_b) is expected to set in. Thus, despite ignorance of the precise value of L , we are able to determine the leading finite-size behavior of the susceptibility.

APPENDIX C: EVALUATION OF THE SCALING FIELD PARAMETERS FOR HELIUM

We imagine a simple model for helium (^3He or ^4He) in which atoms interact via a pair potential $w^l(r; r^0) = 4J^l(r; r^0)$. We assume that the uid is bounded by a substrate whose particles interact with the helium particles with a pair potential $w^{ls}(r; r^0) = 4J^{ls}(r; r^0)$. Within the lattice gas model for any given configuration C of particles $f_{p_i^1}; p_j^1 g, i \in S, j \in L$ with L and S denoting the region occupied by the helium and substrate particles, respectively, the energy of the uid is given by

$$\begin{aligned} E &= \sum_{i \in S, j \in 2L} w_{ij}^{ls} p_i^s p_j^1 + \frac{1}{2} \sum_{i, j \in 2L} w_{ij}^l p_i^1 p_j^1 \\ &= \frac{1}{4} \sum_{i \in S, j \in 2L} J_{ij}^{ls} p_i^s p_j^1 + \frac{1}{2} \sum_{i, j \in 2L} J_{ij}^l p_i^1 p_j^1; \end{aligned} \quad (\text{C } 1)$$

where $p_j^1 \in \{0, 1\}$ and $p_i^s \in \{0, 1\}$ denote the occupation numbers for the uid and substrate particles, respectively. Since only the part $f_{p_j^1} g$ belonging to the uid becomes critical around T_c and the fluctuations of the particles $f_{p_j^s} g$ belonging to the substrate are unimportant here, one can replace the latter ones by their mean-field values. If the uid is in contact with a particle reservoir with a given (excess) chemical potential

and temperature T , the partition function for the liquid is

$$\begin{aligned} Z &= \sum_{f_{p_j^1} g} \exp \left[-\frac{1}{4} \sum_{i \in S, j \in 2L} J_{ij}^{ls} p_i^s p_j^1 - \frac{1}{2} \sum_{i, j \in 2L} J_{ij}^l p_i^1 p_j^1 \right] \\ &= \sum_{f_{p_j^1} g} \exp \left[-\frac{1}{4} \sum_{i \in S, j \in 2L} J_{ij}^{ls} p_i^s p_j^1 - \frac{1}{2} \sum_{i, j \in 2L} J_{ij}^l p_i^1 p_j^1 \right] \\ &= \sum_{f_{p_j^1} g} \exp \left[-\frac{1}{4} \sum_{i \in S, j \in 2L} J_{ij}^{ls} p_i^s p_j^1 - \frac{1}{2} \sum_{i, j \in 2L} J_{ij}^l p_i^1 p_j^1 \right]; \end{aligned} \quad (\text{C } 2)$$

where $p_i^s = \langle p_i^s \rangle$. Since the solid substrate is only weakly influenced by its surface, we assume $\langle p_i^s \rangle = p_s = \text{const.}$ in S so that

$$\begin{aligned} Z &= \sum_{f_{p_j^1} g} \exp \left[-\frac{1}{4} \sum_{i \in S, j \in 2L} J_{ij}^{ls} p_i^s p_j^1 - \frac{1}{2} \sum_{i, j \in 2L} J_{ij}^l p_i^1 p_j^1 \right] \\ &= \sum_{f_{p_j^1} g} \exp \left[-\frac{1}{4} \sum_{i \in S, j \in 2L} J_{ij}^{ls} p_i^s p_j^1 - \frac{1}{2} \sum_{i, j \in 2L} J_{ij}^l p_i^1 p_j^1 \right]; \end{aligned} \quad (\text{C } 3)$$

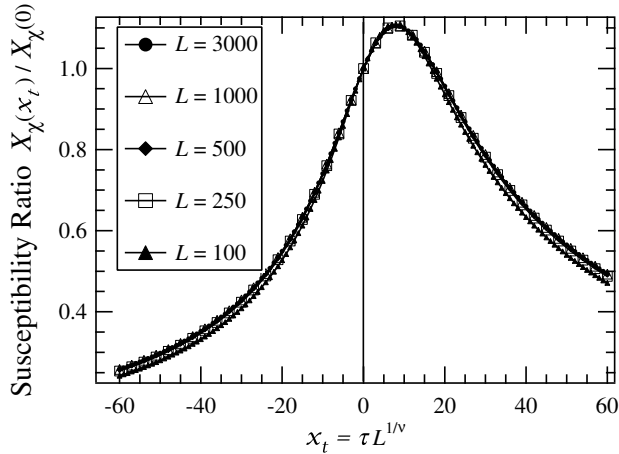


FIG. 15: The finite-size susceptibility for $L = 3000, L = 1000, L = 500, L = 250$, and $L = 100$ normalized to its value at $T = T_c$. The amplitude of the surface magnetic field is rescaled in such a way that $h_{w,ls} = \bar{L} = \text{const}$ for all values of L .

By modeling the pair potentials as

$$J_{ij}^l = J^l (1 + \epsilon_i \epsilon_j \epsilon_i^+ \epsilon_j^+) (\epsilon_i \epsilon_j - 1);$$

and

$$J_{ij}^{ls} = J^{ls} \epsilon_i \epsilon_j \epsilon_i^+ \epsilon_j^+ (\epsilon_i \epsilon_j - 1)$$

one finds for $\sum_i J_{ij}^{ls}$:

$$\begin{aligned}
X_{i2S_1=2} J_{ij}^{1;s} &= J^{1;s} X_{i2S_1=2} \frac{1}{Z_1} \frac{1}{Z_1} = J^{1;s} \frac{X_{i2S_1=2}^2}{Z_1} \frac{1}{Z_1} \\
&= J^{1;s} \int_0^1 dr_1 \int_0^1 dr_2 \int_0^1 dr_d \frac{1}{[(z_j + r_1)^2 + r_2^2 + r_3^2 + \frac{2}{d} r^{(d+1)s}=2]} \\
&= J^{1;s} \frac{(d-1)=2}{s} \frac{\frac{1+s}{2}}{\frac{d+s}{2}} Z_j^{-s}; \quad (C4)
\end{aligned}$$

where $z_j = 1$ characterizes the distance of the particle p_j from the boundary with the half space $S_{1=2}$ occupied by the substrate. We consider the fluid particles to be in the region $0 \leq z \leq L$, where L is the width of the film confined between the two surfaces. Therefore, the partition function is

$$Z = \frac{1}{f_p^3 g} \exp \left\{ 4 \sum_{j=1}^L \sum_{i=1}^L J_{ij}^1 p_j^1 + 2 \sum_{i,j=1}^L J_{ij}^1 p_i^1 p_j^1 \right\} A^5; \quad (C5)$$

i.e., the system is equivalent to one with a spatially varying chemical potential $\mu_j = V_j$ acting on a particle p_j at a distance $z_j + 1, 0 \leq z_j \leq L$, from the left boundary surface and at a distance $(L + 1 - z_j)$ from the right one where $V_j = V(z_j)$ is given by the superposition

$$V(z) = v_s (z + 1)^{-s} + (L + 1 - z)^{-s}; \quad (C6)$$

with

$$v_s = 4 \frac{(d-1)=2}{s} \frac{\frac{1+s}{2}}{\frac{d+s}{2}} J^{1;s}; \quad (C7)$$

In the current article we choose such boundary conditions that $\phi(0) = \phi(L) = 1$, where $\phi(z) = h_j^1$. This is known as (+;+) boundary conditions. The pressure p in the fluid as a function of $f_j g$ and T follows from $p = \beta_j^{-1} \ln Z$, where β_j is the number of lattice sites in the region L . The critical properties of this model can be directly derived from the known critical behavior of the corresponding magnetic system that one obtains under the transformation $m_i = 2p_i - 1$, where $m_i \in [-1, 1]$. One arrives at

$$p = \frac{1}{2} \beta_j^{-1} \ln \left\{ \sum_{j=1}^L \sum_{i=1}^L J_{ij}^1 m_j + \sum_{i,j=1}^L J_{ij}^1 m_i m_j \right\} f; \quad (C8)$$

where f is the free energy of the magnetic system

$$f = \ln \sum_{\{m\}} \exp \left\{ 4 \sum_{j=1}^L m_j h_j + \frac{1}{2} \sum_{i,j=1}^L K_{ij} m_i m_j \right\}; \quad (C9)$$

where

$$K_{ij} = J_{ij}^1; \quad \text{and} \quad h_j = \frac{1}{2} \sum_{i=1}^L K_{ij}; \quad (C10)$$

The mean-field critical properties of the model (C9) are well known. The critical exponents are $\beta = \gamma = 1/2$, $\nu = 1$ and for the uniform system the critical point is at $fh = 0$; $K_c^{-1} = \sum_{ij} K_{ij} g$. At the critical point $\langle m_i \rangle_c = m_c = 0$. Thus, for the fluid system we derive that the corresponding critical point is at $fh = K_c$; $\mu_c = \mu_c g$, where $\mu_c = 2 \sum_{i,j} J_{ij}^1$ while at this point $\langle p_i \rangle_c = \mu_c = 1/2$. With the help of μ_c and μ_c the corresponding expressions for h_j can be rewritten in the form

$$\begin{aligned}
h_j &= \frac{1}{2} (\mu_c) \frac{1}{2} V_j + 4 \sum_{i=1}^L J_{ij}^1 \mu_c \\
&= \frac{1}{2} (\mu_c) + \frac{2 \frac{(d-1)=2}{s} J^{1;s}}{\frac{d+s}{2}} J^1 \mu_c \\
&\quad (z_j + 1)^{-s} + (L + 1 - z_j)^{-s}; \quad (C11)
\end{aligned}$$

From Eq. (C11) (see also [31]) one identifies that

$$h_{w;s} = 2 \frac{(d-1)=2}{s} \frac{\frac{1+s}{2}}{\frac{d+s}{2}} (\sum_{ij} J_{ij}^{1;s} \mu_c J^1); \quad (C12)$$

The equation of the magnetization profile (2.2) also directly follows from Eq. (C9). Denoting $m_i = \langle m_i \rangle$ one obtains

$$m_i = \tanh^4 \left\{ \sum_{j=1}^L K_{ij} m_j + h_j \right\}; \quad (C13)$$

Taking into account that $\mu_c = 1/2$ one can rewrite m_i in the form $m_i = 2 \mu_i - 1 = (\mu_i - \mu_c) \mu_c$ and, thus Eq. (C13) takes the form

$$\frac{\mu_i - \mu_c}{\mu_c} = \tanh^4 \left\{ \sum_{j=1}^L K_{ij} \frac{\mu_j - \mu_c}{\mu_c} + h_j \right\}; \quad (C14)$$

In what follows we take the ^3He or ^4He atoms to be constrained by an Au substrate. Then, according to Refs. [32, 33, 34] $v_s \approx 270 \text{ meV \AA}^3 = r_0^3$, where r_0 is the distance between the helium atom and the Au surface. We will assume that r_0 is the same as the distance between the ^3He or ^4He atoms (but being different for ^3He and ^4He cases, respectively). It is clear that r_0 provides the scale of the length of the unit cell of

the lattice on which we consider the fluid embedded. An estimation of r_0 can be obtained from some general data for ^3He or ^4He . The critical density of ^3He is $\rho_c = 0.01375 \text{ mol/cm}^3 = 0.04145 \text{ g/cm}^3$ [35], while for ^4He it is $\rho_c = 0.017399 \text{ mol/cm}^3 = 0.0690 \text{ g/cm}^3$ [36, 37], wherefrom one easily derives that at the critical point one has $8.28 \cdot 10^{27}$ particles/ m^3 for ^3He and $1.38 \cdot 10^{28}$ particles/ m^3 for ^4He . This leads to the conclusion that the space "allocated" for one particle is of the order of 120.77 \AA^3 for ^3He and of the order of 72.55 \AA^3 for ^4He , i.e. the size of one ^3He atom at the critical point is of the order of 4.9 \AA while for ^4He it is 4.2 \AA . Thus, for v_s one has $v_s = 2.3 \text{ m eV} = 3.68 \cdot 10^{22} \text{ J}$ for ^3He and $v_s = 3.6 \text{ m eV} = 5.82 \cdot 10^{22} \text{ J}$ for ^4He . For T near the critical temperature $T_c = 3.3 \text{ K}$ of ^3He [35] one has $k_B T_c = 4.55 \cdot 10^{23} \text{ J}$ and thus $\rho_c = 2.2 \cdot 10^{22} \text{ J}^{-1}$ with $\rho_c v_s = 8.1$. For ^4He $T_c = 5.2 \text{ K}$ [36, 37] and therefore $k_B T_c = 7.17 \cdot 10^{23} \text{ J}$, $\rho_c = 1.4 \cdot 10^{22} \text{ J}^{-1}$, and $\rho_c v_s = 8.1$. Taking into account that the atomic weight of Au is 196.97 u , whereas its density is 19.3 g/cm^3 and having in mind that the atomic weight of ^3He is 3 u and that the atomic weight of ^4He is 4 u (where $\text{u} = 1.6605 \cdot 10^{-27} \text{ kg}$ is the atomic mass unit), it is easy to verify that the number density of Au is 7.1 times larger than the number density of the ^3He and 5.7 times larger than that of ^4He at the critical point of the respective fluid. Since within the mean-field theory, the number density of both ^3He and ^4He at their respective bulk critical points is $\rho_c = 1/2$, we obtain that $\rho_s = 3.55$ for ^3He films and $\rho_s = 2.85$ for ^4He films. As an estimate of J^{ls} one immediately derives from Eq. (C 7) (for $d = s = 3$) the result that that $J^{ls} = 4.95 \cdot 10^{23} \text{ J}$ for ^3He and that $J^{ls} = 9.75 \cdot 10^{23} \text{ J}$ for ^4He . Next, neglecting the contribution due to J^1 , i.e. the interaction between the atoms of ^3He and also between the atoms of ^4He , one finds that $h_{w,s} = \frac{1}{2} \rho_c v_s = 4.05$ both for ^3He and ^4He films, i.e. the surface field is, indeed, relatively large and cannot be neglected.

Next, we justify the approximation made for J^1 . Within the mean-field approximation we have $\rho_c J^1 = 0.160$. Thus, from the experimentally known value of ρ_c we conclude that $J^1 = 7.3 \cdot 10^{24} \text{ J}$ for ^3He and $J^1 = 1.14 \cdot 10^{23} \text{ J}$ for ^4He . Note that these estimates are very close to those based on the general expectation that $k_B T_c = J^1$, which leads to $J^1 = 10^{23} \text{ J}$. Therefore, $J^{ls} = J^1 = 6.6$ for ^3He and $J^{ls} = J^1 = 8.5$ for ^4He , i.e. the interactions of the atoms of ^3He and ^4He with the Au substrate are much stronger than the interactions between them selves. If, nevertheless, one insists on tak-

ing these interactions into account a simple calculation shows that $h_{w,s}$ changes from $h_{w,s} = 4.05$ to $h_{w,s} = 3.96$ for ^3He and from $h_{w,s} = 4.05$ to $h_{w,s} = 3.97$ for ^4He . Summarizing, one can conclude that the surface field has almost the same value for both the ^3He and ^4He films bounded by Au surfaces, and thus one can predict that the finite-size behavior of their finite-size susceptibilities for a given fixed L will be practically indistinguishable for both fluids.

We finish this Appendix by briefly commenting on the correlation length amplitudes for the correlation lengths

$$\xi(T) = \xi(T \rightarrow T_c; h = 0) = \xi_0 \xi_j$$

and

$$h(h) = \xi(T_c; h \neq 0) = \xi_{0,h} \xi_j = :$$

One can show that in the case of a van der Waals fluid-potential the amplitude ξ_0 of the second moment correlation length is [31]

$$\xi_0 = \frac{\frac{1}{2} P}{\frac{2}{r} \frac{r^2}{1+r^{d+1}}} \Big|_{r=1}^{\infty} : \quad (\text{C 15})$$

Furthermore one has

$$\xi_0 = \xi_0^P = \frac{P}{2}; \quad \text{and} \quad \xi_{0,h} = \xi_0^R = \frac{R}{3}. \quad (\text{C 16})$$

The numerical evaluation of the sum (C 15) for $d = s = 3$ in the case of a simple cubic lattice then gives $\xi_0 = 0.635 \text{ a}$. Taking into account that, as we derived above, $a = 4.9 \text{ \AA}$ for ^3He and $a = 4.2 \text{ \AA}$ for ^4He we obtain that $\xi_0 = 3.11 \text{ \AA}$ for ^3He and that $\xi_0 = 2.67 \text{ \AA}$ for ^4He . Of course the procedure used to calculate the above numbers constitutes a very strong approximation and one shall not expect to reproduce the best known values of these quantities. Nevertheless, the comparison with the known data reported in the literature $\xi_0 = 2.71 \text{ \AA}$ [24, 38] for ^3He , and $\xi_0 = 2.0 \text{ \AA}$ [39] for ^4He , shows that the above results are not too bad. One straightforward way to improve the above approximation is to consider the fluid embedded not on a simple cubic but on a body centered cubic lattice which is probably "closer" to the reality since then the atoms are more closely packed. For such a lattice we obtain $\xi_0 = 0.574 \text{ a}$, and thus $\xi_0 = 2.811 \text{ \AA}$ for ^3He , and $\xi_0 = 2.409 \text{ \AA}$ for ^4He . These results are indeed essentially close to the ones obtained by using much more elaborate methods [24, 38, 39].

- [1] K. Binder, in Phase Transitions and Critical Phenomena, edited by C. Domb and J. L. Lebowitz (Academic, London, 1983), Vol. 8, p. 2.
 [2] H. W. Diehl, in Phase Transitions and Critical Phenomena, edited by C. Domb and J. L. Lebowitz (Academic, London, 1986), Vol. 10, p. 76.

- [3] M. Pleimling, J. Phys. A. 37, R79 (2004).
 [4] S. Dietrich, in Phase Transitions and Critical Phenomena, edited by C. Domb and J. L. Lebowitz (Academic, London, 1988), Vol. 12, p. 1.
 [5] D. Jasnow, in Phase Transitions and Critical Phenomena, edited by C. Domb and J. L. Lebowitz (Academic,

- London, 1986), Vol. 10.
- [6] M. E. Fisher, in *Proceedings of the 1970 Enrico Fermi school of physics, Varena, Italy, Course No LI*, edited by M. S. Green (Academic, New York, 1971), p. 1.
 - [7] M. Barber, in *Phase Transitions and Critical Phenomena*, edited by C. Domb and J. L. Lebowitz (Academic, London, 1983), Vol. 8, p. 145.
 - [8] V. Privman, in *Finite Size Scaling and Numerical Simulation of Statistical Systems*, edited by V. Privman (World Scientific, Singapore, 1990), p. 1.
 - [9] J. G. Brankov, D. M. Danchev, and N. S. Tonchev, *The Theory of Critical Phenomena in Finite-Size Systems - Scaling and Quantum Effects* (World Scientific, Singapore, 2000).
 - [10] R. Evans, U. Marini Bettolo Marconi, and P. Tarazona, *J. Chem. Phys.* **84**, 2376 (1986); A. O. Parry and R. Evans, *J. Phys. A* **25**, 275 (1992); K. Binder and D. P. Landau, *J. Chem. Phys.* **96**, 1444 (1992).
 - [11] K. Binder, D. P. Landau, and A. M. Ferrenberg, *Phys. Rev. Lett.* **74**, 298 (1995); A. O. Parry, *J. Phys. A* **25**, 257 (1992); K. Binder, R. Evans, D. P. Landau, and A. M. Ferrenberg, *Phys. Rev. E* **53**, 5023 (1996).
 - [12] K. Binder, D. P. Landau, and M. Muller, *J. Stat. Phys.* **110**, 1411 (2003).
 - [13] D. Danchev and J. Rudnick, *Eur. Phys. J. B* **21**, 251 (2001).
 - [14] D. Danchev, *Eur. Phys. J. B* **23**, 211 (2001).
 - [15] H. Chamati and D. Danchev, *Eur. Phys. J. B* **26**, 89 (2002).
 - [16] D. Danchev, M. Krech, and S. Dietrich, *Phys. Rev. E* **67**, 066120 (2003).
 - [17] N. Tonchev, *Physics of Particles and Nuclei* **36**, Suppl. 1, S82 (2005).
 - [18] D. Danchev, H. W. Diehl, D. Gruneberg, *Phys. Rev. E* **73**, 016131 (2006).
 - [19] L. Peliti and S. Leibler, *J. Phys. C.: Solid State Phys.* **16**, 2635 (1983).
 - [20] K. Binder and D. P. Landau, *Physica A* **177**, 483 (1991).
 - [21] J. Zinn-Justin, *Quantum Field Theory and Critical Phenomena* (Clarendon, Oxford, 2002).
 - [22] R. F. Kayser and H. J. Raveche, *Phys. Rev. A* **29**, 1013 (1984).
 - [23] M. Ley-Koo and M. S. Green, *Phys. Rev. A* **23**, 2650 (1981).
 - [24] F. Zhong, M. Barnatz and I. Hahn, *Phys. Rev. E* **67**, 021106 (2003).
 - [25] J. V. Sengers, in *Phase Transitions*, edited by M. Levy, J.-C. Le Guillow, and J. Zinn-Justin, *NATO Advanced Study Institute Series B*, Vol. 72 (Plenum, New York, 1982), p. 95.
 - [26] A. Maciolek, A. Drzewinski, and P. Bryk, *J. Chem. Phys.* **120**, 1921 (2004).
 - [27] H. Nakanishi and M. E. Fisher, *Phys. Rev. Lett.* **49**, 1565 (1982).
 - [28] H. Nakanishi and M. E. Fisher, *J. Chem. Phys.* **78**, 3279 (1983).
 - [29] M. Krech, *Phys. Rev. E* **56**, 1642 (1997).
 - [30] E. Cheng and M. W. Cole, *Phys. Rev. B* **38**, 987 (1988).
 - [31] D. Danchev, F. Schlesener and S. Dietrich, to be published.
 - [32] G. Vidali and M. W. Cole, *Surface Science* **110**, 10 (1981).
 - [33] E. Zaremba and W. Kohn, *Phys. Rev. B* **13**, 2270 (1976).
 - [34] E. Zaremba and W. Kohn, *Phys. Rev. B* **15**, 1769 (1977).
 - [35] C. Pittman, T. Doiron, and H. Meyer, *Phys. Rev. B* **20**, 3678 (1979).
 - [36] E. W. Lemmon, M. O. McLinden, and D. G. Friend, in *NIST Chemistry WebBook*, NIST Standard Reference Database Number 69, edited by W. G. Mallard and P. J. Linstrom (National Institute of Standards and Technology, Gaithersburg, MD, 2000). See <http://webbook.nist.gov>
 - [37] P. R. Roach, *Phys. Rev.* **170**, 213 (1968).
 - [38] Y. Garrabos, F. Palencia, C. Lecoutre, and C. Erkey, *Phys. Rev. E* **73**, 026125 (2006).
 - [39] A. B. Kogan and H. Meyer, *J. Low Temp. Phys.* **110**, 899 (1998).